Maintaining structural and functional homeostasis of the *Drosophila* respiratory epithelia requires stress-modulated JAK/STAT activity

Xiao Niu[1, 2], Christine Fink[1], Kimberley Kallsen[3, 4], Leizhi Shi[1, 5], Viktoria Mincheva[1], Sören Franzenburg[6], Ruben Prange[1], Iris Bruchhaus[7], Judith Bossen[1, 8], Holger Heine[2, 8], Thomas Roeder[1, 8]

[1]Kiel University, Zoology, Dept. of Molecular Physiology, Kiel, Germany

[2]Current address: Weifang Medical University, College of Life Science and Technology, Weifang, China

[3]Research Center Borstel – Leibniz Lung Center, Div. of Innate Immunity, Borstel, Germany

[4]Current address: Boehringer Ingelheim, Ingelheim, Germany

[5]Department of Thoracic Surgery, Linyi People's Hospital, Linyi, Shandong, 276000, China

[6]Kiel University, IKMB, Kiel, Germany

[7]Bernhard Nocht Institute for Tropical Medicine, Hamburg, Germany

[8]German Center for Lung Research, Airway Research Center North, Kiel, Germany

Highlights

1. JAK/STAT signaling is active in the entire *Drosophila* respiratory system in all developmental stages.

2. The signaling pathway is indispensable for the survival of the tracheal cell.

3. Overactivation of the signaling has significant effects on tracheal development and also displays a human disease-associated phenotype in *Drosophila* trachea.

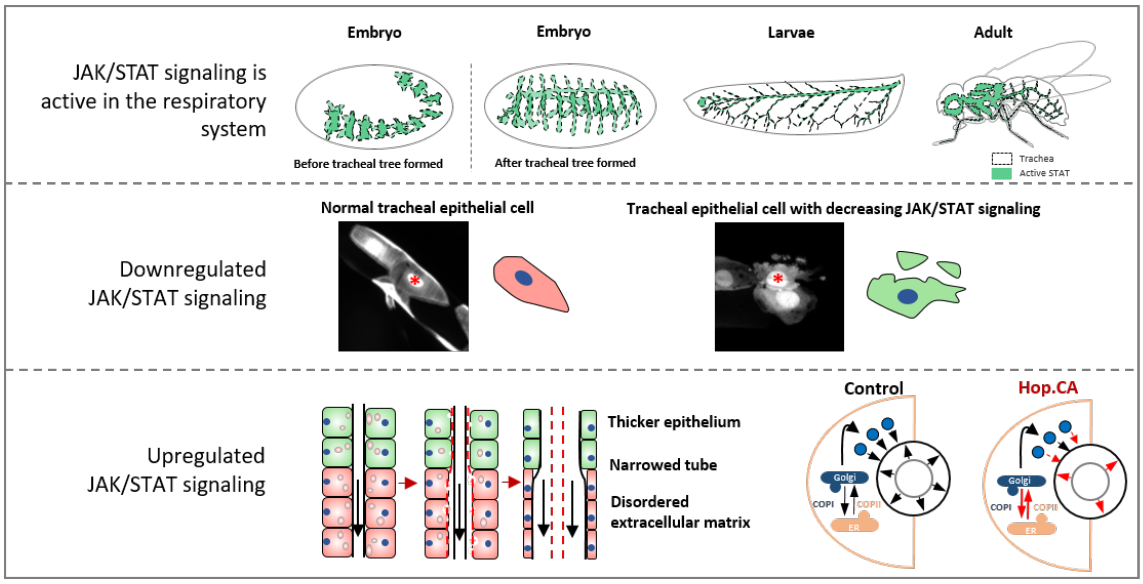

Summary

Signaling mediated by the Janus kinase (JAK)/Signal Transducer and Activator of Transcription (STAT) pathway is critical for maintaining cellular and functional homeostasis in the lung. Thus, chronically activated JAK/STAT signaling is causally associated with lung diseases such as lung cancer, asthma, and chronic obstructive pulmonary disease. To elucidate the molecular processes that transform increased JAK/STAT signaling in airway epithelial cells into the known pathological states, we used a highly simplified model system, the fruit fly *Drosophila melanogaster*. Here, the JAK/STAT pathway is permanently active in almost all airway cells and responds to airborne stressors with increased activity. Silencing of this signaling pathway in epithelial cells resulted in apoptosis. Since the above-mentioned lung diseases are commonly associated with increased JAK/STAT signaling, we assessed this by its ectopic activation in the respiratory epithelium of *Drosophila*. This intervention triggered cell-autonomous structural changes in epithelial cells. These structural changes included phenotypes associated with asthma, namely, thickening of the epithelium, substantial narrowing of the air-conducting space, and impairment of the secretory epicuticular structure of the tracheae. Pharmacological manipulation of JAK/STAT signaling reversed this pathological phenotype. Transcriptomic analyses revealed that several biological processes were affected, which is consistent with the impairment of junction protein trafficking also observed in this study. These results indicate that balanced JAK/STAT signaling is essential for the functionality of the

48 respiratory epithelium and, by extension, the entire organ. In contrast, chronic
49 overactivation of this signaling leads to massive structural changes that are closely
50 associated with pathologies typical of chronic inflammatory lung diseases.

Introduction

The Janus kinase (JAK)/signal transducer and activator of transcription (STAT) signaling system is of central importance for several critical physiological processes such as development, tissue homeostasis, and immune responses (Philips et al., 2022; Rawlings et al., 2004). Signal transduction via this pathway is straightforward and allows environmental factors to directly influence transcriptional activity, linking key biological processes to the environment (Kiu and Nicholson, 2012). Deregulation of this pathway is linked to numerous human diseases, with cancer and inflammatory pathologies being particularly prominent (Hu et al., 2021; Milara et al., 2018). JAK/STAT signaling acts downstream of a plethora of cytokines that transmit immune-related information, acting as a central integration hub in almost all cells of the lung (Yew-Booth et al., 2015)(Villarino et al., 2017). Signaling via this pathway is essential during organ development and for maintaining tissue and immune homeostasis of the fully differentiated lung. Here, JAK/STAT signaling is required to cope with stressors, infection, and damage (Jin et al., 2018; Kida et al., 2008; Major et al., 2020; Makris et al., 2017; Tadokoro et al., 2014). Given the importance of JAK/STAT signaling in the lung, it is predictable that decreased or increased signaling via this pathway leads to pathologies. Whereas reduced JAK/STAT signaling corresponds with impaired repair capacities (Tadokoro et al., 2014), increased JAK/STAT signaling is associated with a plethora of chronic lung diseases including asthma, chronic obstructive pulmonary disease (COPD), idiopathic pulmonary fibrosis (IPF), and

lung cancer (Dutta et al., 2014; Georas et al., 2021; Milara *et al.*, 2018; Yew-Booth *et al.*, 2015). Despite its simple general organization, the JAK/STAT signaling pathway in vertebrates shows multiple redundancies, parallels, and convergences; a situation that is further complicated since these signaling pathways may act differently in different cell types of the same organ (Hu *et al.*, 2021; Morris et al., 2018; Villarino *et al.*, 2017). Therefore, models with a much simpler JAK/STAT signaling pathway and a less complex cellular composition in the airways should help to elucidate the effects of deregulated JAK/STAT signaling, especially in airway epithelial cells. *Drosophila melanogaster* can be used for this task, as only one receptor (Domeless), one JAK kinase (Hopscotch), and one STAT transcription factor (STAT92E) are present (Arbouzova and Zeidler, 2006; Zeidler and Bausek, 2013). This low level of redundancy offers the unique advantage to study the generic relevance of JAK/STAT signaling. Furthermore, the use of *Drosophila* allows focusing exclusively on the airway epithelium, a resident cell population playing a central role in the orchestration of organ homeostasis, but also for developing chronic pathologies. In the tracheal system of *Drosophila*, the lung's functional equivalent, there is so far only information on the relevance of JAK/STAT signaling during embryonic development and the formation of the adult tracheal system (Brown et al., 2001; Perrimon and Mahowald, 1986; Powers and Srivastava, 2019). A lack of JAK/STAT signaling during very early phases of tracheal development impairs tracheal development including cell movement and elongation, as well as invagination processes that lead to tube formation (Brown et al.,

2001; Isaac and Andrew, 1996). During the development of the vertebrate lung, very similar processes are operative (Nogueira-Silva et al., 2006; Piairo et al., 2018). In recent years, *Drosophila* served as a model for numerous human diseases (Pandey and Nichols, 2011) including those of the lung (Bossen et al., 2021; Levine and Cagan, 2016; Prange et al., 2018; Roeder et al., 2009; Roeder et al., 2012).

The current study aimed to elucidate the general importance of JAK/STAT signaling in the airways and understand how chronic deregulation of this pathway in airway epithelial cells results in pathological outcomes. Applying a tailored *Drosophila* model, we could not only show that JAK/STAT signaling is required to prevent apoptosis of airway epithelial cells but that a wide variety of stressors increased signaling via this pathway significantly. Ectopic activation on the other hand, leads to massive structural changes that drastically limit airway epithelial functionality. Using this model, we demonstrated that balanced JAK/STAT signaling in airway epithelia is imperative to prevent the development of pathology and that pharmacological intervention at precisely this point is excellent for addressing it.

Results

Activation of the JAK/STAT pathway occurs in a wide variety of organs and can easily and reliably be visualized in *Drosophila* using transcriptional reporters. Here, the activity of the pathway (Fig. 1A) is visualized by a STAT92E-promoter-dependent GFP-based reporter

approach (Bach et al., 2007). It was already known that the JAK/STAT pathway is strongly activated in the trachea during embryogenesis and it could be assumed to be important for tracheal development (Bach et al., 2007). However, the exact pattern of its activation is still unclear. To fill this gap of knowledge, we analyzed the *STAT92E*-reporter activity concurrently with *btl>LacZ.nls* (Shiga et al., 1996), which specifically labels the trachea. Activation of the *STAT92E-GFP* reporter was pronounced in a central region in the trachea, mainly in the transverse connective area (Fig. 1B–D). To evaluate if the JAK/STAT pathway also operates in a functional airway epithelium under control conditions, we used the *STAT92E-GFP* reporter line to monitor pathway activity in the larval tracheal system (Fig. 1E). JAK/STAT activity was relatively low in the posterior zone of the trachea (Fig. 1F), the tenth tracheal metamere (Tr10), where cells progressively undergo apoptosis in response to trachea metamorphosis (Bosch et al., 2015; Chen and Krasnow, 2014). However, JAK/STAT activity was much stronger in regions such as Tr2, the spiracular branch (SB), and the dorsal branch (DB) than in nearby areas (Fig. 1G and H). In these areas with high JAK/STAT activity, cells re-enter the cell cycle at this developmental stage (Guha et al., 2008; Sato et al., 2008; Weaver and Krasnow, 2008). We next evaluated if JAK/STAT activity is observed in airway epithelial cells of adults. The same approach detected substantial reporter activity in airway epithelial cells of fully developed adults (Fig. 1I). The JAK/STAT pathway was active throughout the entire tracheal system. In addition, we evaluated the expression of the three *upds* in the larval trachea. Experiments using the corresponding

enhancer-*Gal4* lines demonstrated that especially *upd2* was highly expressed in the tracheal system (Fig. S1).

The JAK/STAT pathway responds to stressful stimuli

To investigate whether external, stress-associated stimuli can affect JAK/STAT signaling in airway epithelia, we exposed the just-described reporter lines to these stimuli. We focused on airborne stressors and exposed both larvae and adults to them. Here, the administration of cold air (cold), hypoxia, and cigarette smoke (CSE) boosted the activity of the JAK/STAT pathway in airway epithelial cells (Figure 2A and 2C) of both larval and adult animals. A quantitative evaluation of the induced fluorescent signals showed that these increases were statistically significant (Fig. 2C).

Then we expanded the analysis of the effects of airborne stressors to include the ligands of the signaling system. We found that one of the three ligands, *upd*, did not show any expression independent of the situation (data not shown). In contrast, the expression of *upd2* and *upd3* were induced by external stimuli, for *upd2* only by CSE, for *upd3* by CSE and hypoxia (Fig. S2). The activity of the *STAT92E-GFP* reporter was induced exactly in the region where also the ligand showed enhanced expression. For further analyses, we focused on the most responsive *upd* gene, namely *upd3*. Expression of *upd3* was low in the tracheal cells of larvae or adult animals that lived under control conditions but could easily be observed in all these tracheal cells when the animals were exposed to external stimuli (Fig. 2B and 2D).

JAK/STAT signaling is essential for the survival of airway epithelial cells

To evaluate the relevance of the JAK/STAT pathway in the *Drosophila* respiratory system, we blocked its activity in the trachea by driving the expression of a dominant-negative isoform of Domeless (*Dome.DN*) using the trachea-specific *btl-Gal4* driver. As a result, some animals developed to the larval stage (Fig. 3A), but all died before reaching the pupal stage. Microscopic analysis of surviving larvae showed that the dorsal trunk (DT) was absent (Fig. 3B'). Time-lapse imaging of embryos experiencing trachea-specific *Dome.DN* expression revealed that all tracheal segments were fused, however, the DT subsequently separated (Fig. 3C). STAT92E-RNAi was used to confirm this kind of effects on trachea. A detailed analysis of the effects caused by constitutive *Dome.DN* expression was performed using a mosaic approach (Wu et al., 2006). Here, driving expression in a mosaic fashion by *vvl-FLP*, *CoinFLP-Gal4* changed the morphology of the affected cells. These cells appear to undergo apoptosis (Fig. 3D). Apoptosis of these affected cells was confirmed by the detection of Dcp1 in exactly these cells, which is a hallmark of apoptosis (Fig. 3E-F). Apoptosis was induced to an even greater extent (and faster) in progenitor cells of the larval tracheal system, where Dcp1-positive cells were observed on day 1 after induction of *Dome.DN* expression (Fig. 3G-I).

Increased JAK/STAT signaling induced cell-autonomous structural changes in epithelial cells

We tested the effects of ectopic activation of the JAK/STAT pathway induced by expression of the ligand (*upd3*) or a constitutively active JAK-allele (*Hop.CA*) on tracheal development. These animals died prematurely at the embryo or larval stage (Fig. 4A-B). Microscopic analysis of larvae and embryos showed that the tracheal segment separated at the larval stage (Fig. 4E), however, the disconnection of segments was due to the failure of their fusion at the beginning of tracheal development (Fig. 4C and 4D). In contrast with animals that ectopically expressed *upd3*, more animals expressing *Hop.CA* exhibited an intact tracheal tree (Fig. 4D). However, they all died at the first larval stage, which indicates that JAK/STAT signaling can influence both tracheal formation and growth.

To elucidate the effects of JAK/STAT upregulation in the tracheal system, we employed the temperature inducible Gal4/Gal80[ts] system which could initiate activation of the signaling pathway at different time points during larval development (Fig. S3A). We first tested the effects of inhibition of the tracheal JAK/STAT pathway induced by ectopic expression of *Dome.DN* on the animals. Ectopic expression was initiated at three time points during larval development (Fig. S3B). Larval mortality was higher, the earlier expression was initiated. No larvae survived to the pupal stage (Fig. S3C). On the other hand, activation of JAK/STAT signaling induced by ectopic expression of *upd3* or *Hop.CA* led to lower levels of larval death (Fig. S3B). In both cases, no pupae developed into adults (Fig. S3C). Furthermore, we analyzed the effects of this intervention on tracheal structure. Whereas *Dome.DN* overexpression elicited only minor effects on tracheal structure, *upd3*

189 or *Hop.CA* overexpression caused substantial epithelial thickening (Fig. 4F). Quantitative
190 measurements revealed that ectopic overexpression of *Hop.CA* greatly increased
191 epithelial thickness up to more than 10-fold (Fig. 4H). Experiments involving mosaic
192 expression of *Hop.CA* driven by *vvl-FLP*, *CoinFLP-Gal4, UAS-EGFP (vvl-coin)* demonstrated
193 that this effect was cell-autonomous. In the same trachea, cells that expressed *Hop.CA*
194 were much thicker than their neighboring cells that did not express *Hop.CA* (Fig. 4I). The
195 thicker epithelium could be caused by increased cell volume, increased cell number, or
196 reduced tube surface area. To elucidate the mechanisms underlying this structural
197 response, we analyzed the phenotype in more detail. Consequently, the length-thickness
198 (Fig. 4G) product mirrored the findings made when assessing thickness (Fig. 4J). However,
199 the number of cells in the dorsal trunk of Tr8, or DT8 of the trachea with manipulated
200 JAK/STAT signaling was like that in matching controls (Fig. 4K). Hence, the thickening was
201 due to an increase in cell volume, not an increase in cell number. To determine if this
202 thickening is an artifact caused by the isolation method, we directly fixed the trachea *in*
203 *situ* or isolated it in cell culture medium with the same osmolarity as the hemolymph. The
204 same thickening was observed in both cases (Fig. S4). To quantify the time course of this
205 thickening, we subjected the trachea to different treatment regimens prior to analysis. At
206 least 2 days of ectopic expression were necessary to induce this phenotype (Fig. S5).

207 The effects of activating the JAK/STAT pathway on the epithelium were time-dependent
208 (Fig. 4F). To determine if a weaker expression of *Hop.CA* induces similar phenotypes, we

used another trachea-specific Gal4-driver, namely, *nach-Gal4* (also called *ppk4-Gal4*). In the *nach-Gal4* line, *Gal4* is expressed from the late embryo stage. Moreover, it is strongly expressed in the early L1 and late L2 stages, at which point expression is stronger than that driven by *btl-Gal4* but is weakly expressed at other larval stages (Liu et al., 2003; Wagner et al., 2009). Microscopic analysis of the trachea showed that weak expression of *Hop.CA* in the trachea promoted epithelial thickening (Fig. 4L). However, epithelial thickening after 4 days of *Hop.CA* induction was lower in *nach>Hop.CA* than in *btl>Hop.CA* (Fig. 4M). On the other hand, weakly driven *upd3* expression in the trachea resulted in identical increases in the thickness as those observed using *btl-Gal4* (Fig. 4N). Finally, we used the same driver to inhibit JAK/STAT signaling in the trachea by expressing *Dome.DN*. Animals died prematurely at the larval stage and their trachea were filled with liquid, demonstrating that functionality was strongly impaired (Fig. 4O). As activation of the IMD pathway by PGRP-LC overexpression induced a very similar phenotype (Wagner et al., 2021), we tested the hypothesis that both, IMD- and JAK/STAT- activation act in the same pathway. Therefore, we activated the IMD-pathway (via PGRP-LC overexpression) while concurrently silencing JAK/STAT signaling (via STAT92e-RNAi) and found no rescue of the thickening phenotype (Fig. 4P).

Treatment with various JAK inhibitors (Roskoski, 2016) reversed epithelial thickening induced by ectopic overexpression of *Hop.CA* in the trachea (Fig. 4Q). Treatment with Baricitinib, Oclacitinib, or Filgotinib reduced epithelial thickening by more than 60%

229 therewith showing its potential in interfering with the JAK/STAT signaling pathway and the
230 induced pathological situations (Fig. 4R).

231 **Transcriptomic response to enhanced JAK/STAT signaling**

232 To investigate the molecular mechanisms underlying the effects of chronic JAK/STAT
233 activation on the airways, we performed mRNA-sequencing analysis of tracheal cells
234 expressing *Hop.CA* in third instar larvae. The validity of this experimental procedure was
235 controlled by measuring transcript levels of of *hopscotch* (including *Hop.CA*) and *Socs36E*
236 (one of the best-characterized STAT92E target genes) (Bach et al., 2007), which were
237 upregulated 35-fold and 2.7-fold, respectively ($p < 10^{-12}$) (Fig. S6B). Principal component
238 analysis of biological replicates separated control and overexpression samples into
239 different groups (Fig. S6A, inner region). Finally, the analysis revealed that the expression
240 of 2004 genes was statistically significantly regulated ($p < 0.05$; > 1.5 fold up or down),
241 with 1128 downregulated genes and 876 upregulated genes ($p < 0.05$). A circular heatmap
242 of a subgroup of them under more stringent conditions with 707 differentially expressed
243 genes ($p < 0.01$ and fold change > 2) is shown (Fig. S6A). Moreover, we analyzed changes
244 in expression upon ectopic silencing of the JAK/STAT pathway using *Dome.DN*. A Venn
245 diagram revealed that there was a statistically significant overlap in the cohorts of genes
246 regulated by both interventions (Fisher's exact test, $p < 0.0001$; Fig. S6C).

247 To further elucidate the molecular mechanisms functioning in the thickened epithelium,
248 we performed promotor scan studies and functional enrichment analyses. Genes with the

highest rates of induction supported by the lowest p-values were subjected to promoter scanning (Pscan) analysis. Putative genes directly regulated by the JAK/STAT pathway were identified (Tab. 1 and Tab. 2). Among these highly regulated genes, the largest group contained genes that encoded products involved in innate immunity, including seven antimicrobial peptide genes (*IM1 (BomS1), IM2 (BomS2), IM4 (Dso1), IM14 (Dso2), CG5791 (BomBc3), CG5778 (BomT3),* and *Drs*). All these antimicrobial peptides, except for Drs, contain one or two CXXC regions. These CXXC-containing peptides belong to the family of Bomanins, whose expression is highly induced following bacterial or fungal infection, and high levels of the corresponding mature peptides are found in the hemolymph of infected flies (Lindsay et al., 2018).

Next, we analyzed all significantly regulated genes based on KEGG and GO annotations. Six KEGG pathways and ten categories in GO analysis were enriched in the comparison of the *Hop.CA* expressing trachea compared with the matching controls (Tab. S1 and Fig. 5A-B). One striking feature of the epithelium with chronically activated JAK/STAT signaling was the induced expression of genes involved in “vesicle-mediated transport processes” (Fig. 5A). GO enrichment analysis demonstrated that this term was shared by 32 regulated genes. All these genes were upregulated, except for one (*CG5946*). However, according to a Pscan analysis, these genes did not seem to be direct JAK/STAT targets since predicted STAT92E promoter binding sites were not enriched in the corresponding promoter regions (Tab. S2 and S3). The transcript levels of genes that could be assigned for the term

"epicuticle development" were reduced. Here, fifty-five genes relevant to cuticle development were regulated, of which 40 were downregulated. In addition, other biological processes such as "muscle cell differentiation", "cellular protein-containing complex assembly", "RNA processing, translation", and "detection of chemical stimuli" were significantly enriched. In the latter three categories, the number of upregulated genes was like the number of downregulated genes. A schematic representation of the different biological processes superimposed on a scheme of an epithelial cell is shown (Fig. 5B). These alterations at the transcript level were reminiscent of the finding in allergic airways disease, where the expression of cell adhesion molecules or their transport to the membrane of airway epithelial cells are impaired (Bonnelykke et al., 2014; Giridhar et al., 2016; Heijink et al., 2020; Xiao et al., 2011). To test this, we analyzed mouse lungs of an experimental asthma model based on the usage of OVA for sensitization (Fig. 5C-E). Those animals of the asthma model displayed typical structural changes in the airways (Fig. 5D) and the relevant proinflammatory cytokines showed the anticipated increase in expression (Fig. 5E). Consistent with the effects observed in *Drosophila*, the expression of genes involved in the biological process vesicle transport were significantly affected in those mice with an induced experimental allergic airway disease (Fig. 5F) and most of these differentially expressed genes were increased.

Impairment of protein transport in airway epithelial cells with chronically enhanced JAK/STAT signaling

To evaluate if the transport capacities in the *Drosophila* airway epithelial cells is improved or impaired, we focused on two peripheral membrane-associated proteins involved in cell-cell interactions. These proteins were Coracle (Cora), a component of the septate junctions, and Armadillo (Arm), a component of the adherens junctions. Both proteins depend on vesicle transport to reach their final destinations (Lock and Stow, 2005; Oshima and Fehon, 2011) (Fig. 6A). Immunofluorescence analysis of *Hop.CA*-overexpressing animals revealed that Arm and Cora accumulated in the cytoplasm, which is indicative of dysfunctional vesicle transport (Fig. 6B–E).

The transcriptome data revealed that “cuticle development” was another GO that was enriched. This process depends on the secretory abilities of epithelial cells in the larval trachea. Here, chitin-rich structures, called taenidia, are believed to make tubes flexible as well as sufficiently strong in order to avoid collapse (Glasheen et al., 2010). The chitin structure in the trachea showed a strongly reduced degree of regularity in *Hop.CA*-expressing animals compared with control ones (Fig. 7A-B). Chitin staining revealed that the highly organized structure of the chitinous intima was almost completely lost in *Hop.CA*-expressing animals (Fig. 7A’’ and 7B’’). The mosaic analysis demonstrated that the trachea was structurally disorganized exactly at those sites where *Hop.CA* was expressed (Fig. S7).

We propose a simple model that explains structural phenotypes mainly based on the impaired vesicle-mediated transport and the lack of adhesion-associated proteins to the

membrane, which is in line with previous findings about this biological process (Jayaram et al., 2008; Tsarouhas et al., 2007) (Fig. 7C). Lumen narrowing is another phenotype that might be caused by the dysfunction of the process which could be observed in our study as well. This is prominently seen when epithelial cells expressed *Hop.CA* at very high levels, as indicated by strong green fluorescence (Fig. 7D-E and Fig. S4).

Discussion

The present study aimed to clarify the generic role of the JAK/STAT pathway in the respiratory epithelium. We mainly used the fruit fly *Drosophila* because it has ideal characteristics for conducting this study. The unique features of this model allowed us to focus on the essentials, namely the entirety of the signaling pathway and its importance in respiratory epithelial cells. The JAK/STAT signaling pathway in mammals has a degree of redundancy and parallelism in all its levels, rarely observed in other signaling systems. However, this exceptionally high degree of parallelism hampers determing the significance of JAK/STAT signaling per se and whether it differs substantially from signaling through individual cytokines or receptors. As mentioned earlier, the Drosophila JAK/STAT signaling pathway is simple, allowing targeted manipulation. Here, we showed that 1) JAK/STAT signaling exhibited tonic activity in almost all respiratory epithelial cells, 2) that exposure to airborne stressors such as hypoxia or cigarette smoke enhanced its activity, 3) that blocking JAK/STAT signaling induces apoptosis, and that 4) ectopic activation in epithelial

cells induced several phenotypes reminiscent of those found in chronic inflammatory lung diseases such as epithelial thickening or narrowing of the airways. The main results 1-3 are thematically very closely related. The tonus of JAK/STAT signaling shown in embryonic, larval, and adult airway epithelia suggests that this cellular function is essential as it probably ensures the survival of these epithelial cells. JAK/STAT signaling is required to maintain the cellular identity of airway epithelial cells (D'Amico et al., 2018) and is important for the response to airway epithelial injury and epithelial cell survival (Juncadella et al., 2013; Paris et al., 2020; Tadokoro *et al.*, 2014). This agrees with our studies, which revealed that blockade of the signaling pathway leads to apoptosis of airway epithelial cells of flies. Furthermore, it implies that the JAK/STAT pathway plays a central role in homeostatic processes in this organ, which also appears to be the case in mammalian airway epithelia. Perturbation of JAK/STAT signaling induces apoptosis in cell lines derived from airway epithelia (Zheng et al., 2016), and this is particularly relevant for tissues and cells that can still divide or grow (Quinton and Mizgerd, 2011). This ability to grow might be one reason for the high susceptibility of Drosophila airway epithelial cells to the blockade of JAK/STAT signaling. Thus, cytokines that activate the JAK/STAT signaling pathway act as survival factors, especially when repair mechanisms are operative. Functional JAK/STAT signaling is also required for regenerative processes after epithelial damage (Kida *et al.*, 2008; Paris *et al.*, 2020; Tadokoro *et al.*, 2014), the response to infections (Matsuzaki et al., 2006), and the reaction to hyperoxia (Hokuto et al., 2004).

This indicates that JAK/STAT signaling in mammalian airway epithelial cells and the *Drosophila* trachea is particularly relevant for a protective reaction to stressful stimuli. In *Drosophila*, we observed a basal level of JAK/STAT signaling in these cells, and this signaling was further activated in response to very strong stressors such as chronic exposure to smoke particles. An organ-autonomous JAK/STAT signaling system seems to be operative, composed of the cytokines Upd2 and Upd3 and the activated signaling pathway induced in the same regions of the tracheal system. A comparable, stress-induced system was identified in the intestinal epithelium of flies, where highly stressful insults targeting absorptive enterocytes induce the production and release of the cytokine Upd3 (Jiang et al., 2009; Miguel-Aliaga et al., 2018). In contrast to the intestine, where cytokines produced by stressed enterocytes induce the proliferation of stem cells to replenish the enterocyte pool, stem cells are not involved in the tracheal response.

Although a threshold level of JAK/STAT signaling is required for the functionality and survival of airway epithelial cells, excessive activation of this signaling is associated with several lung diseases such as lung cancer, acute lung injury, asthma, pulmonary fibrosis, and COPD (Adnot et al., 2019; Chen et al., 2021; D'Amico *et al.*, 2018; Dutta *et al.*, 2014; Gao et al., 2004; Milara *et al.*, 2018; Parakh et al., 2021; Prele et al., 2012; Simeone-Penney et al., 2007; Yew-Booth *et al.*, 2015; Zhang et al., 2012). The ectopic activation of JAK/STAT signaling in the fly's airway epithelium induced major structural changes, mainly to the architecture of tracheal cells. The mosaic analysis demonstrated that this effect was cell

autonomous. These structural changes of the trachea are reminiscent of those observed in asthma, COPD, acute lung injury, and lung cancer. Structural changes that permit fulfillment of the original function of epithelial cells are hallmarks of the epithelial-to-mesenchymal transition. In lung cancer, the epithelial-to-mesenchymal transition depends on JAK/STAT signaling (Liu et al., 2014).

Ectopic JAK/STAT pathway activation also induced complex transcriptomic alterations in airway epithelial cells. These changes also affected immune-relevant genes, such as those encoding antimicrobial peptides, mainly from the Bomanin family. This dependency of antimicrobial responses on JAK/STAT signaling is also seen in the mammalian airway epithelium (Choi et al., 2013; Simeone-Penney *et al.*, 2007). However, chronically activated JAK/STAT signaling perturbed secretory processes and the formation of extracellular structures. The extracellular matrix defects caused by *Hop.CA* overexpression are reminiscent of the pathophysiology of the aforementioned chronic lung diseases that involve responses to acute or chronic injury (Fahy and Dickey, 2010). Therefore, attempts to enhance the repair capacities of epithelial cells by inducing structural changes via excessive JAK/STAT signaling would also perturb normal cellular functions, such as the transport of junction proteins to the membrane. This would lead to a reduced barrier function of the epithelium, which is a hallmark of chronic lung diseases such as asthma and COPD (Georas and Rezaee, 2014; Gon and Hashimoto, 2018; Heijink et al., 2012). We

388 also observed epicuticular changes, which considerably influenced the structure of the
389 whole organ. However, it is difficult to identify an equivalent response in vertebrates.

390 Furthermore, our finding that the JAK/STAT signaling pathway operates in airway epithelial
391 cells of embryos, larvae, and adults implies that it plays a central role in these cells at all
392 developmental stages. The JAK/STAT pathway is involved in the embryonic development
393 of the tracheal system (Hombria and Sotillos, 2013). We clarified the sequence of
394 developmental steps in which this signaling pathway plays a central role. The JAK/STAT
395 signaling pathway is particularly relevant for developing and maintaining the dorsal trunk.
396 It is a matter of debate, whether JAK/STAT signaling is essential for mammalian lung
397 development. However, the prevailing view that JAK/STAT signaling is not essential for
398 embryonic lung development (Tadokoro et al., 2014) has been challenged by recent
399 studies (Piairo et al., 2018). Although JAK/STAT signaling is essential for different aspects
400 of tracheal development, the major focus of the current study was to understand its role
401 in maintaining homeostasis in the fully functional airway epithelium.

402 The JAK/STAT pathway is an excellent target for therapeutic intervention in many lung
403 diseases, including asthma, COPD, acute lung injury, idiopathic pulmonary fibrosis, and
404 lung cancer (Athari, 2019; Loh et al., 2019; Milara *et al.*, 2018; Severgnini et al., 2004; Song
405 et al., 2011; Yew-Booth *et al.*, 2015). We demonstrated that pharmacological interference
406 of the JAK/STAT signaling pathway reverted the structural phenotype observed upon
407 ectopic activation of this signaling and, consequently flies survived. This shows that the

Drosophila model is not only suitable to study the structural effects of excessive JAK/STAT signaling and the underlying molecular mechanisms but also to screen compounds and thereby identify novel therapeutic strategies. Moreover, the intrinsic architecture of the *Drosophila* system allows the prediction that the major site of action is the airway epithelium, thus implying that inhalation would be the ideal route of drug administration in a therapeutic setting.

It should be remembered that the vertebrate lung and insect trachea are not homologous. Nevertheless, both airway systems share a high degree of similarity regarding their development, physiology, innate immunity, and operative signaling systems (Andrew and Ewald, 2010; Bergman et al., 2017). Therefore, the fruit fly is a valuable tool for studying genes associated with a great variety of chronic lung diseases, including asthma, COPD, and lung cancer (Bossen et al., 2019; Kallsen et al., 2015; Levine and Cagan, 2016; Prange *et al.*, 2018; Roeder *et al.*, 2009; Roeder *et al.*, 2012). This simple model can be used as part of an experimental toolbox to elucidate the role of JAK/STAT signaling in the airways and the effects of chronic deregulation of this signaling. In addition, it provides a readily accessible experimental system that is amenable to pharmacologic interventions and allows hypotheses and intervention strategies to be easily tested.

Material and Methods

***Drosophila* strains and husbandry**

STAT92E-GFP was used to monitor the activation of the pathway (Bach et al., 2007); the Gal4-UAS system (Brand and Perrimon, 1993) was used to target ectopic expression to the tracheal system. Gal4 drivers used were: *btl-Gal4, UAS-GFP* on the 3rd chromosome, and *btl-Gal4, UAS-GFP* on the 2nd chromosome (obtained from the Leptin group, Heidelberg, Germany); *upd2-Gal4*; *upd3-Gal4* (Prange et al., 2018); *nach-Gal4* (Liu et al., 2003). The UAS responders included: *UAS-LacZ.nls* (BDSC 3956), *UAS-domeΔcyt2.1* (*UAS-Dome.DN*) and *UAS-Hop.CA* (*UAS-hopTumL*) were obtained from N. Perrimon (Brown et al., 2001; Harrison et al., 1995). The *UAS-upd3* was constructed in our lab. *TubP-Gal80[ts]* (BDSC 7018) was obtained from the Bloomington stock center. Unless otherwise stated, the flies were raised on standard medium at 25 °C with 50–60% relative humidity under a 12:12 h light/dark cycle as described earlier (Fink et al., 2016).

Coin-FLP expression system

Vvl-FLP/CyO; btl-moe.mRFP (BDSC 64233), *tubP-Gal80[ts]* and *CoinFLP-Gal4, UAS-2xEGFP* (BDSC 58751) were used to construct animals for the tracheal mosaic analysis. Ventral veins lacking (*vvl*) was expressed in larval tracheal clones that covered approximately 30 to 80% of the trachea (Bosch *et al.*, 2015; Chen and Krasnow, 2014). The genotype of the flies was *vvl-FLP*, *CoinFLP-Gal4*, *UAS-2xEGFP*/*CyO* (*vvl-coin*) and *vvl-FLP*, *CoinFLP-Gal4*, *UAS-2xEGFP*/*CyO*; *tub-Gal80[ts]* (*vvl-coin.ts*).

446 **Developmental viability**

447 For developmental viability of eggs, the eggs were collected overnight and were not
448 physically handled in any way. The number of the hatched eggs and the pupae were
449 counted starting from two days after the collection. Each group has 4 replicates that
450 included more than 20 eggs. For developmental viability of larvae, *tub-Gal80[ts]* was used
451 to limit UAS responder expression at the larvae stage. Animals were raised at 18 °C to keep
452 the UAS responder gene silent. Larvae at different instar stages were transferred to a new
453 medium at 29 °C. In this study, usually 4 replicates were performed with 30 larvae. The
454 stage of larvae was determined via the appearance of anterior spiracles.

455 **Determination of epithelial thickness**

456 The trachea of L2 and L3 Larvae were carefully dissected from the posterior side of the
457 body in PBS. The isolated trachea were immersed in 50% glycerol and digital images were
458 captured within 15 min. L2 Larvae were distinguished from L3 larvae by the appearance
459 of anterior spiracles. The relative ages of L3 larvae were inferred from the size of the
460 animal. 30 larvae were used in each group and specimens were analyzed by Image J.

461 **Drug application in *Drosophila***

462 JAK inhibitors (Baricitinib #16707, Oclacitinib #18722, Filgotinib #17669 - Cayman
463 Chemicals, Michigan, USA) were diluted in DMSO [100 mM]. For later application the
464 inhibitors were diluted 1:10 in 100% EtOH. We used 20 µl of each diluted inhibitor for 2

ml of concentrated medium (5% yeast extract, 5% corn flour, 5% sucrose, 1% low-melt agarose, 1 ml of 10% propionic acid and 3 ml of 10% Nipagin). The eggs of each crossing have been applicated on the modified medium and kept at 20 °C until the larvae reach the L2 stage. Afterwards they were incubated at 30 °C for 2 days to induce the *btl-Gal4, UAS-GFP; tub-Gal80[ts]* (*btl.ts*)–driver. The trachea of L3 Larvae were carefully dissected from the posterior side of the body in PBS. Isolated trachea was immersed in 50% glycerol and digital images were captured in 15 min. 10 larvae were used for each group.

Experimental design for hypersensitivity pneumonitis in mice

Experimental design for hypersensitivity pneumonitis contains two processes, sensitization and challenge of mice with ovalbumin (Sigma Aldrich, A5503). The protocol refers to the protocol that (Daubeuf and Frossard, 2013) described with a few modifications. 8 week-old Balb/C mice were sensitized with intraperitoneal injections of 20 μg of OVA emulsified in aluminum hydroxide in a total volume of 1 ml on days 7 and 14, followed by 3 consecutive challenges each day by exposure to OVA or PBS aerosol for 30 min. Mice were sacrificed 24 h following the final challenge. The left lungs were collected for histological analysis and the superior lobes were dissected for RNA analysis. 6 mice per group were used in this experiment and 4 mice were randomly selected in each group for analyses. Total mRNA sequencing, data processing, and statistical analysis were performed by Genesky (Shanghai, China). The experimental protocols were

485 approved by the Animal Care and Protection Committee of Weifang Medical University
486 (2021SDL418).

487 **AB-PAS staining and immunofluorescence analysis of mouse lung**

488 Mice were sacrificed in excess CO_2 gas. The lungs of euthanized mice were inflated by
489 intratracheal injection of cold 4% paraformaldehyde and then were fixed and embedded
490 in paraffin as described in (Baligar et al., 2016). AB-PAS staining, and Immunofluorescence
491 analysis were supported by Servicebio (Wuhan, China). All sections were photographed
492 using a microscope slide scanner (Pannoramic MIDI: 3Dhistech). The materials and
493 methods could be found at the following link https://www.servicebio.cn/data-
494 detail?id=3040&code=MYYGSYBG and https://www.servicebio.cn/data-detail?id=35
495 95&code=RSSYBG. We list the main reagents here: AB-PAS solution set (Servicebio,
496 G1049), Anti-CD11b (Servicebio, GB11058) and DAPI (Servicebio, G1012-10ML).

497 **Time-lapse microscopy**

498 All images were acquired using a ZEISS Axio Image Z1 and a ZEISS LSM 880 fluorescent
499 microscope (INST 257/591-1 FUGG). Embryos were dechorionated in 3% sodium
500 hypochlorite and immersed in Halocarbon oil 700 (Sigma Aldrich, 9002-83-9). Then the
501 embryos were imaged after stage 15 when the tracheal tree formed at 3 hours intervals.
502 40 embryos were investigated in each group.

503 **Cigarette smoke and hypoxic exposure**

All cigarette smoke exposure experiments were carried out in a smoking chamber, attached to a diaphragm pump. Common research 3R4F cigarettes (CTRP, Kentucky University, Lexington, USA) were used for all experiments. The vials containing animals were capped with a monitoring grid to allow the cigarette smoke to diffuse into the vial. For long-time smoke experiments, L2 larvae were exposed to smoke three times a day for 30 min each, on two consecutive days. For heavy smoke experiments, L3 larvae were exposed to smoke of 2 cigarettes for 45 min, which led to about 35-50% mortality. To study the effects of hypoxia on the activity of JAK/STAT signaling pathway, larvae were exposed to long-term hypoxia and short-term hypoxia separately. For long-term hypoxia experiments, L2 larvae were exposed to 5% oxygen three times a day for 30 min each, on two consecutive days. For short-term hypoxia experiments, L3 larvae were exposed to 1% oxygen once for 5 hours. At least 20 animals in 4 vials were investigated in each group.

Immunohistochemistry of *Drosophila* trachea

Larvae were dissected by ventral filleting and fixed in 4% paraformaldehyde for 30 min. Embryos were staged according to Campos-Ortega and Hartenstein (Campos-Ortega and Hartenstein, 1997) and fixed in 4% formaldehyde for 30 min. Immunostaining followed standard protocols as described earlier (Jeon et al., 2008; Levi et al., 2006). GFP signals were amplified by immunostaining with polyclonal rabbit anti-GFP (used at 1:500, Sigma-Aldrich, Merck KGaA, Darmstadt, Germany, SAB4301138). 40-1a (used at 1:50, DSHB, Iowa City, USA) was used to detect Beta-galactosidase. Coracle protein was detected with a

524 monoclonal mouse anti-coracle antibody (used at 1:200, DSHB, Iowa City, USA, C566.9).
525 Armadillo protein was detected with a monoclonal mouse anti-armadillo antibody (DSHB,
526 US, N2 7A1, used at 1:500). A monoclonal rabbit Cleaved Drosophila Dcp1 (used at 1:200,
527 Cell Signaling, Frankfurt/M, Germany, #9578) was used to detect apoptotic cells.
528 Secondary antibodies used were: Cy3-conjugated goat-anti-mouse, Cy3-conjugated goat-
529 anti-rabbit, Alexa488-conjugated goat-anti-mouse (used at 1:500, Jackson
530 Immunoresearch, Dianova, Hamburg, Germany), Alexa488-conjugated goat-anti-rabbit
531 (used at 1:500, Cell signaling, Frankfurt/M, Germany, #9578). Tracheal chitin was stained
532 with 505 star conjugated chitin-binding probe (NEB, Frankfurt/M, Germany, used at 1:300).
533 Nuclei were stained with 4',6-Diamidino-2-Phenylindole, Dihydrochloride (DAPI) (Roth,
534 Karlsruhe, Germany, 6843). 30 specimens were investigated in each group. Specimens
535 were analyzed and digital images were captured either with a confocal (Zeiss LSM 880,
536 Oberkochen, Germany) or a conventional fluorescence microscope (ZEISS Axio Imager Z1,
537 Zeiss, Oberkochen, Germany), respectively.

538 **RNA isolation and RNA sequencing**

539 For the gene expression analysis of 3rd instar larvae trachea, animals were dissected in
540 cold PBS and isolated trachea transferred to RNA Magic (BioBudget, Krefeld, Germany)
541 and processed essentially as described earlier (Prange et al., 2018) with slight
542 modifications. The tissue was homogenized in a Bead Ruptor 24 (BioLab products,
543 Bebensee, Germany) and the RNA was extracted by using the PureLink RNA Mini Kit

(Thermo Fisher, Waltham, MA, USA) for phase separation with the RNA Magic reagent. An additional DNase treatment was performed following the on-column PureLink DNase treatment protocol (Thermo Fisher, Waltham, MA, USA).

Sequencing libraries were constructed using the TruSeq stranded mRNA kit (Illumina, San Diego, USA) and 50 bp single-read sequencing was performed on an Illumina HiSeq 4000 with 16 samples per lane. Resulting sequencing reads were trimmed for low-quality bases and adapters using the fastq Illumina filter (http://cancan.cshl.edu/labmembers/gordon /fastq_illumina_filter/) and cutadapt (version 1.8.1) (Martin, 2011). Transcriptomics analysis including gene expression values and differential expression analysis was done using CLC Genomics Workbench. The detailed protocols can be obtained from the CLC Web site (http://www. clcbio.com/products/clc-genomics-workbench). *Drosophila melanogaster* reference genome (Release 6) (Hoskins et al., 2015) was used for mapping in this research.

The transcription factor binding site enrichment and the Gene Ontology enrichment analyses of the differentially expressed genes were carried out using Pscan (http://159.149.160.88/pscan/) and online GO enrichment analysis (http://geneontology.org/), respectively. We chose -450- 50 bases of the annotated transcription start site of the genes as the transcription factor binding sites for enrichment analysis. The analysis performed with the TFBSs matrices that is available in the JASPAR databases (version

Jaspar 2018_NR). Data were visualized through the circos software http://circos.ca/software/.

Statistics and reproducibility

We did not use statistical methods to predetermine sample sizes but the sample sizes used in this study are similar or higher as those used in previous studies (Proske et al., 2021; Wagner *et al.*, 2021). Specific approaches to randomly allocate samples to groups were not used and the experiments were not performed in a blinded design. No data were excluded from the analysis. Prism (GraphPad version 7) was used for statistical analyses and the corresponding tests used are listed in the figure legends.

Acknowledgments

Funding

This work was funded by the DFG as part of the CRC 1182 and by funding of the CLSM (INST 257/591-1 FUGG). Moreover, Xiao Niu received funds from the Chinese Scholarship Council and Weifang Medical University. Leizhi Shi received funds from the Linyi People's Hospital.

References

Adnot, S., Lipskaia, L., and Bernard, D. (2019). The STATus of STAT3 in Lung Cell Senescence? Am J Respir Cell Mol Biol *61*, 5-6. 10.1165/rcmb.2019-0013ED.

Andrew, D.J., and Ewald, A.J. (2010). Morphogenesis of epithelial tubes: Insights into tube formation, elongation, and elaboration. Dev Biol *341*, 34-55. 10.1016/j.ydbio.2009.09.024.

Arbouzova, N.I., and Zeidler, M.P. (2006). JAK/STAT signalling in Drosophila: insights into conserved regulatory and cellular functions. Development *133*, 2605-2616. 10.1242/dev.02411.

Athari, S.S. (2019). Targeting cell signaling in allergic asthma. Signal Transduct Target Ther *4*, 45. 10.1038/s41392-019-0079-0.

Bach, E.A., Ekas, L.A., Ayala-Camargo, A., Flaherty, M.S., Lee, H., Perrimon, N., and Baeg, G.H. (2007). GFP reporters detect the activation of the Drosophila JAK/STAT pathway in vivo. Gene Expr Patterns *7*, 323-331. 10.1016/j.modgep.2006.08.003.

Baligar, P., Pokhrel, S., and Mukhopadhyay, A. (2016). Experimental Liver Fibrosis and Intrasplenic Transplantation of CD45+ Bone Marrow Cells. Bio-protocol *6*, e1972. 10.21769/BioProtoc.1972.

Bergman, P., Seyedoleslami Esfahani, S., and Engstrom, Y. (2017). Drosophila as a Model for Human Diseases-Focus on Innate Immunity in Barrier Epithelia. Curr Top Dev Biol *121*, 29-81. 10.1016/bs.ctdb.2016.07.002.

Bonnelykke, K., Sleiman, P., Nielsen, K., Kreiner-Moller, E., Mercader, J.M., Belgrave, D., den Dekker, H.T., Husby, A., Sevelsted, A., Faura-Tellez, G., et al. (2014). A genome-wide association study identifies CDHR3 as a susceptibility locus for early childhood asthma with severe exacerbations. Nat Genet *46*, 51-55. 10.1038/ng.2830.

Bosch, J.A., Tran, N.H., and Hariharan, I.K. (2015). CoinFLP: a system for efficient mosaic screening and for visualizing clonal boundaries in Drosophila. Development *142*, 597-606. 10.1242/dev.114603.

Bossen, J., Uliczka, K., Steen, L., Neugebauer, P., Mai, M.M., Fink, C., Stracke, F., Heine, H., and Roeder, T. (2021). Driver mutations in major lung cancer oncogenes can be analyzed in Drosophila models. ALTEX *38*, 235-244. 10.14573/altex.1912131.

Bossen, J., Uliczka, K., Steen, L., Pfefferkorn, R., Mai, M.M., Burkhardt, L., Spohn, M., Bruchhaus, I., Fink, C., Heine, H., and Roeder, T. (2019). An EGFR-Induced Drosophila Lung Tumor Model Identifies Alternative Combination Treatments. Mol Cancer Ther *18*, 1659-1668. 10.1158/1535-7163.MCT-19-0168.

Brand, A.H., and Perrimon, N. (1993). Targeted gene expression as a means of altering cell fates and generating dominant phenotypes. Development *118*, 401-415.

Brown, S., Hu, N., and Hombria, J.C. (2001). Identification of the first invertebrate interleukin JAK/STAT receptor, the Drosophila gene domeless. Curr Biol *11*, 1700-1705. 10.1016/s0960-9822(01)00524-3.

Campos-Ortega, J.A., and Hartenstein, V. (1997). The Embryonic Development of Drosophila melanogaster (Springer-Verlag Berlin Heidelberg). 10.1007/978-3-662-22489-2.

Chen, F., and Krasnow, M.A. (2014). Progenitor outgrowth from the niche in Drosophila trachea is guided by FGF from decaying branches. Science *343*, 186-189. 10.1126/science.1241442.

Chen, X., Miao, M., Zhou, M., Chen, J., Li, D., Zhang, L., Sun, A., Guan, M., Wang, Z., Liu, P., et al. (2021). Poly-L-arginine promotes asthma angiogenesis through induction of FGFBP1 in airway epithelial cells via activation of the mTORC1-STAT3 pathway. Cell Death Dis *12*, 761. 10.1038/s41419-021-04055-2.

Choi, S.M., McAleer, J.P., Zheng, M., Pociask, D.A., Kaplan, M.H., Qin, S., Reinhart, T.A., and Kolls, J.K. (2013). Innate Stat3-mediated induction of the antimicrobial protein Reg3gamma is required for host defense against MRSA pneumonia. J Exp Med *210*, 551-561. 10.1084/jem.20120260.

D'Amico, S., Shi, J., Martin, B.L., Crawford, H.C., Petrenko, O., and Reich, N.C. (2018). STAT3 is a master regulator of epithelial identity and KRAS-driven tumorigenesis. Genes Dev *32*, 1175-1187. 10.1101/gad.311852.118.

Daubeuf, F., and Frossard, N. (2013). Acute Asthma Models to Ovalbumin in the Mouse. Curr Protoc Mouse Biol *3*, 31-37. 10.1002/9780470942390.mo120202.

Dutta, P., Sabri, N., Li, J., and Li, W.X. (2014). Role of STAT3 in lung cancer. JAKSTAT *3*, e999503. 10.1080/21623996.2014.999503.

Fahy, J.V., and Dickey, B.F. (2010). Airway mucus function and dysfunction. N Engl J Med *363*, 2233-2247. 10.1056/NEJMra0910061.

Fink, C., Hoffmann, J., Knop, M., Li, Y., Isermann, K., and Roeder, T. (2016). Intestinal FoxO signaling is required to survive oral infection in Drosophila. Mucosal Immunol *9*, 927-936. 10.1038/mi.2015.112.

Gao, H., Guo, R.F., Speyer, C.L., Reuben, J., Neff, T.A., Hoesel, L.M., Riedemann, N.C., McClintock, S.D., Sarma, J.V., Van Rooijen, N., et al. (2004). Stat3 activation in acute lung injury. J Immunol *172*, 7703-7712. 10.4049/jimmunol.172.12.7703.

Georas, S.N., Donohue, P., Connolly, M., and Wechsler, M.E. (2021). JAK inhibitors for asthma. J Allergy Clin Immunol *148*, 953-963. 10.1016/j.jaci.2021.08.013.

Georas, S.N., and Rezaee, F. (2014). Epithelial barrier function: at the front line of asthma immunology and allergic airway inflammation. J Allergy Clin Immunol *134*, 509-520. 10.1016/j.jaci.2014.05.049.

Giridhar, P.V., Bell, S.M., Sridharan, A., Rajavelu, P., Kitzmiller, J.A., Na, C.L., Kofron, M., Brandt, E.B., Ericksen, M., Naren, A.P., et al. (2016). Airway Epithelial KIF3A Regulates Th2 Responses to Aeroallergens. J Immunol *197*, 4228-4239. 10.4049/jimmunol.1600926.

Glasheen, B.M., Robbins, R.M., Piette, C., Beitel, G.J., and Page-McCaw, A. (2010). A matrix metalloproteinase mediates airway remodeling in Drosophila. Dev Biol *344*, 772-783. 10.1016/j.ydbio.2010.05.504.

Gon, Y., and Hashimoto, S. (2018). Role of airway epithelial barrier dysfunction in pathogenesis of asthma. Allergol Int *67*, 12-17. 10.1016/j.alit.2017.08.011.

Guha, A., Lin, L., and Kornberg, T.B. (2008). Organ renewal and cell divisions by differentiated cells in Drosophila. Proc Natl Acad Sci U S A *105*, 10832-10836. 10.1073/pnas.0805111105.

Harrison, D.A., Binari, R., Nahreini, T.S., Gilman, M., and Perrimon, N. (1995). Activation of a Drosophila Janus kinase (JAK) causes hematopoietic neoplasia and developmental defects. EMBO J *14*, 2857-2865.

Heijink, I.H., Brandenburg, S.M., Postma, D.S., and van Oosterhout, A.J. (2012). Cigarette smoke impairs airway epithelial barrier function and cell-cell contact recovery. Eur Respir J *39*, 419-428. 10.1183/09031936.00193810.

Heijink, I.H., Kuchibhotla, V.N.S., Roffel, M.P., Maes, T., Knight, D.A., Sayers, I., and Nawijn, M.C. (2020). Epithelial cell dysfunction, a major driver of asthma development. Allergy *75*, 1902-1917. 10.1111/all.14421.

Hokuto, I., Ikegami, M., Yoshida, M., Takeda, K., Akira, S., Perl, A.K., Hull, W.M., Wert, S.E., and Whitsett, J.A. (2004). Stat-3 is required for pulmonary homeostasis during hyperoxia. J Clin Invest *113*, 28-37. 10.1172/JCI19491.

Hombria, J.C., and Sotillos, S. (2013). JAK-STAT pathway in Drosophila morphogenesis: From organ selector to cell behavior regulator. JAKSTAT *2*, e26089. 10.4161/jkst.26089.

Hoskins, R.A., Carlson, J.W., Wan, K.H., Park, S., Mendez, I., Galle, S.E., Booth, B.W., Pfeiffer, B.D., George, R.A., Svirskas, R., et al. (2015). The Release 6 reference sequence of the Drosophila melanogaster genome. Genome Res *25*, 445-458. 10.1101/gr.185579.114.

Hu, X., Li, J., Fu, M., Zhao, X., and Wang, W. (2021). The JAK/STAT signaling pathway: from bench to clinic. Signal Transduct Target Ther *6*, 402. 10.1038/s41392-021-00791-1.

Isaac, D.D., and Andrew, D.J. (1996). Tubulogenesis in Drosophila: a requirement for the trachealess gene product. Genes Dev *10*, 103-117. 10.1101/gad.10.1.103.

Jayaram, S.A., Senti, K.A., Tiklova, K., Tsarouhas, V., Hemphala, J., and Samakovlis, C. (2008). COPI vesicle transport is a common requirement for tube expansion in Drosophila. PLoS One *3*, e1964. 10.1371/journal.pone.0001964.

Jeon, M., Nguyen, H., Bahri, S., and Zinn, K. (2008). Redundancy and compensation in axon guidance: genetic analysis of the Drosophila Ptp10D/Ptp4E receptor tyrosine phosphatase subfamily. Neural Dev *3*, 3. 10.1186/1749-8104-3-3.

Jiang, H., Patel, P.H., Kohlmaier, A., Grenley, M.O., McEwen, D.G., and Edgar, B.A. (2009). Cytokine/Jak/Stat signaling mediates regeneration and homeostasis in the Drosophila midgut. Cell *137*, 1343-1355. 10.1016/j.cell.2009.05.014.

Jin, H., Ciechanowicz, A.K., Kaplan, A.R., Wang, L., Zhang, P.X., Lu, Y.C., Tobin, R.E., Tobin, B.A., Cohn, L., Zeiss, C.J., et al. (2018). Surfactant protein C dampens inflammation by decreasing JAK/STAT activation during lung repair. Am J Physiol Lung Cell Mol Physiol *314*, L882-L892. 10.1152/ajplung.00418.2017.

Juncadella, I.J., Kadl, A., Sharma, A.K., Shim, Y.M., Hochreiter-Hufford, A., Borish, L., and Ravichandran, K.S. (2013). Apoptotic cell clearance by bronchial epithelial cells critically influences airway inflammation. Nature *493*, 547-551. 10.1038/nature11714.

Kallsen, K., Zehethofer, N., Abdelsadik, A., Lindner, B., Kabesch, M., Heine, H., and Roeder, T. (2015). ORMDL deregulation increases stress responses and modulates repair pathways in Drosophila airways. J Allergy Clin Immunol *136*, 1105-1108. 10.1016/j.jaci.2015.04.009.

Kida, H., Mucenski, M.L., Thitoff, A.R., Le Cras, T.D., Park, K.S., Ikegami, M., Muller, W., and Whitsett, J.A. (2008). GP130-STAT3 regulates epithelial cell migration and is required for repair of the bronchiolar epithelium. Am J Pathol *172*, 1542-1554. 10.2353/ajpath.2008.071052.

Kiu, H., and Nicholson, S.E. (2012). Biology and significance of the JAK/STAT signalling pathways. Growth Factors *30*, 88-106. 10.3109/08977194.2012.660936.

Levi, B.P., Ghabrial, A.S., and Krasnow, M.A. (2006). Drosophila talin and integrin genes are required for maintenance of tracheal terminal branches and luminal organization. Development *133*, 2383-2393. 10.1242/dev.02404.

699 Levine, B.D., and Cagan, R.L. (2016). Drosophila Lung Cancer Models Identify Trametinib plus Statin as
700 Candidate Therapeutic. Cell Rep *14*, 1477-1487. 10.1016/j.celrep.2015.12.105.
701 Lindsay, S.A., Lin, S.J.H., and Wasserman, S.A. (2018). Short-Form Bomanins Mediate Humoral Immunity in
702 Drosophila. J Innate Immun *10*, 306-314. 10.1159/000489831.
703 Liu, L., Johnson, W.A., and Welsh, M.J. (2003). Drosophila DEG/ENaC pickpocket genes are expressed in the
704 tracheal system, where they may be involved in liquid clearance. Proc Natl Acad Sci U S A *100*, 2128-2133.
705 10.1073/pnas.252785099.
706 Liu, R.Y., Zeng, Y., Lei, Z., Wang, L., Yang, H., Liu, Z., Zhao, J., and Zhang, H.T. (2014). JAK/STAT3 signaling is
707 required for TGF-beta-induced epithelial-mesenchymal transition in lung cancer cells. Int J Oncol *44*, 1643-
708 1651. 10.3892/ijo.2014.2310.
709 Lock, J.G., and Stow, J.L. (2005). Rab11 in recycling endosomes regulates the sorting and basolateral
710 transport of E-cadherin. Mol Biol Cell *16*, 1744-1755. 10.1091/mbc.e04-10-0867.
711 Loh, C.Y., Arya, A., Naema, A.F., Wong, W.F., Sethi, G., and Looi, C.Y. (2019). Signal Transducer and Activator
712 of Transcription (STATs) Proteins in Cancer and Inflammation: Functions and Therapeutic Implication. Front
713 Oncol *9*, 48. 10.3389/fonc.2019.00048.
714 Major, J., Crotta, S., Llorian, M., McCabe, T.M., Gad, H.H., Priestnall, S.L., Hartmann, R., and Wack, A.
715 (2020). Type I and III interferons disrupt lung epithelial repair during recovery from viral infection. Science
716 *369*, 712-717. 10.1126/science.abc2061.
717 Makris, S., Paulsen, M., and Johansson, C. (2017). Type I Interferons as Regulators of Lung Inflammation.
718 Front Immunol *8*, 259. 10.3389/fimmu.2017.00259.
719 Martin, M. (2011). Cutadapt Removes Adapter Sequences From High-Throughput Sequencing Reads.
720 EMBnet.journal *17*, 10-12. doi.org/10.14806/ej.17.1.200.
721 Matsuzaki, Y., Xu, Y., Ikegami, M., Besnard, V., Park, K.S., Hull, W.M., Wert, S.E., and Whitsett, J.A. (2006).
722 Stat3 is required for cytoprotection of the respiratory epithelium during adenoviral infection. J Immunol
723 *177*, 527-537. 10.4049/jimmunol.177.1.527.
724 Miguel-Aliaga, I., Jasper, H., and Lemaitre, B. (2018). Anatomy and Physiology of the Digestive Tract of
725 Drosophila melanogaster. Genetics *210*, 357-396. 10.1534/genetics.118.300224.
726 Milara, J., Ballester, B., Morell, A., Ortiz, J.L., Escriva, J., Fernandez, E., Perez-Vizcaino, F., Cogolludo, A.,
727 Pastor, E., Artigues, E., et al. (2018). JAK2 mediates lung fibrosis, pulmonary vascular remodelling and
728 hypertension in idiopathic pulmonary fibrosis: an experimental study. Thorax *73*, 519-529.
729 10.1136/thoraxjnl-2017-210728.
730 Morris, R., Kershaw, N.J., and Babon, J.J. (2018). The molecular details of cytokine signaling via the
731 JAK/STAT pathway. Protein Sci *27*, 1984-2009. 10.1002/pro.3519.
732 Nogueira-Silva, C., Santos, M., Baptista, M.J., Moura, R.S., and Correia-Pinto, J. (2006). IL-6 is constitutively
733 expressed during lung morphogenesis and enhances fetal lung explant branching. Pediatr Res *60*, 530-536.
734 10.1203/01.pdr.0000242300.09427.3b.
735 Oshima, K., and Fehon, R.G. (2011). Analysis of protein dynamics within the septate junction reveals a
736 highly stable core protein complex that does not include the basolateral polarity protein Discs large. J Cell
737 Sci *124*, 2861-2871. 10.1242/jcs.087700.
738 Pandey, U.B., and Nichols, C.D. (2011). Human disease models in Drosophila melanogaster and the role of
739 the fly in therapeutic drug discovery. Pharmacol Rev *63*, 411-436. 10.1124/pr.110.003293.

Parakh, S., Ernst, M., and Poh, A.R. (2021). Multicellular Effects of STAT3 in Non-small Cell Lung Cancer: Mechanistic Insights and Therapeutic Opportunities. Cancers (Basel) *13*. 10.3390/cancers13246228.

Paris, A.J., Hayer, K.E., Oved, J.H., Avgousti, D.C., Toulmin, S.A., Zepp, J.A., Zacharias, W.J., Katzen, J.B., Basil, M.C., Kremp, M.M., et al. (2020). STAT3-BDNF-TrkB signalling promotes alveolar epithelial regeneration after lung injury. Nat Cell Biol *22*, 1197-1210. 10.1038/s41556-020-0569-x.

Perrimon, N., and Mahowald, A.P. (1986). l(1)hopscotch, A larval-pupal zygotic lethal with a specific maternal effect on segmentation in Drosophila. Dev Biol *118*, 28-41. 10.1016/0012-1606(86)90070-9.

Philips, R.L., Wang, Y., Cheon, H., Kanno, Y., Gadina, M., Sartorelli, V., Horvath, C.M., Darnell, J.E., Jr., Stark, G.R., and O'Shea, J.J. (2022). The JAK-STAT pathway at 30: Much learned, much more to do. Cell *185*, 3857-3876. 10.1016/j.cell.2022.09.023.

Piairo, P., Moura, R.S., Baptista, M.J., Correia-Pinto, J., and Nogueira-Silva, C. (2018). STATs in Lung Development: Distinct Early and Late Expression, Growth Modulation and Signaling Dysregulation in Congenital Diaphragmatic Hernia. Cell Physiol Biochem *45*, 1-14. 10.1159/000486218.

Powers, N., and Srivastava, A. (2019). JAK/STAT signaling is involved in air sac primordium development of Drosophila melanogaster. FEBS Lett *593*, 658-669. 10.1002/1873-3468.13355.

Prange, R., Thiedmann, M., Bhandari, A., Mishra, N., Sinha, A., Hasler, R., Rosenstiel, P., Uliczka, K., Wagner, C., Yildirim, A.O., et al. (2018). A Drosophila model of cigarette smoke induced COPD identifies Nrf2 signaling as an expedient target for intervention. Aging (Albany NY) *10*, 2122-2135. 10.18632/aging.101536.

Prele, C.M., Yao, E., O'Donoghue, R.J., Mutsaers, S.E., and Knight, D.A. (2012). STAT3: a central mediator of pulmonary fibrosis? Proc Am Thorac Soc *9*, 177-182. 10.1513/pats.201201-007AW.

Proske, A., Bossen, J., von Frieling, J., and Roeder, T. (2021). Low-protein diet applied as part of combination therapy or stand-alone normalizes lifespan and tumor proliferation in a model of intestinal cancer. Aging (Albany NY) *13*, 24017-24036. 10.18632/aging.203692.

Quinton, L.J., and Mizgerd, J.P. (2011). NF-kappaB and STAT3 signaling hubs for lung innate immunity. Cell Tissue Res *343*, 153-165. 10.1007/s00441-010-1044-y.

Rawlings, J.S., Rosler, K.M., and Harrison, D.A. (2004). The JAK/STAT signaling pathway. J Cell Sci *117*, 1281-1283. 10.1242/jcs.00963.

Roeder, T., Isermann, K., and Kabesch, M. (2009). Drosophila in asthma research. Am J Respir Crit Care Med *179*, 979-983. 10.1164/rccm.200811-1777PP.

Roeder, T., Isermann, K., Kallsen, K., Uliczka, K., and Wagner, C. (2012). A Drosophila asthma model - what the fly tells us about inflammatory diseases of the lung. Adv Exp Med Biol *710*, 37-47. 10.1007/978-1-4419-5638-5_5.

Roskoski, R., Jr. (2016). Janus kinase (JAK) inhibitors in the treatment of inflammatory and neoplastic diseases. Pharmacol Res *111*, 784-803. 10.1016/j.phrs.2016.07.038.

Sato, M., Kitada, Y., and Tabata, T. (2008). Larval cells become imaginal cells under the control of homothorax prior to metamorphosis in the Drosophila tracheal system. Dev Biol *318*, 247-257. 10.1016/j.ydbio.2008.03.025.

Severgnini, M., Takahashi, S., Rozo, L.M., Homer, R.J., Kuhn, C., Jhung, J.W., Perides, G., Steer, M., Hassoun, P.M., Fanburg, B.L., et al. (2004). Activation of the STAT pathway in acute lung injury. Am J Physiol Lung Cell Mol Physiol *286*, L1282-1292. 10.1152/ajplung.00349.2003.

781 Shiga, Y., M., T.M., and Hayashi, S. (1996). A nuclear GFP/β-galactosidase fusion protein as a marker for
782 morphogenesis in living Drosophila. Development, Growth & Differentiation *38*, 99-106.
783 doi.org/10.1046/j.1440-169X.1996.00012.x.
784 Simeone-Penney, M.C., Severgnini, M., Tu, P., Homer, R.J., Mariani, T.J., Cohn, L., and Simon, A.R. (2007).
785 Airway epithelial STAT3 is required for allergic inflammation in a murine model of asthma. J Immunol *178*,
786 6191-6199. 10.4049/jimmunol.178.10.6191.
787 Song, L., Rawal, B., Nemeth, J.A., and Haura, E.B. (2011). JAK1 activates STAT3 activity in non-small-cell
788 lung cancer cells and IL-6 neutralizing antibodies can suppress JAK1-STAT3 signaling. Mol Cancer Ther *10*,
789 481-494. 10.1158/1535-7163.MCT-10-0502.
790 Tadokoro, T., Wang, Y., Barak, L.S., Bai, Y., Randell, S.H., and Hogan, B.L. (2014). IL-6/STAT3 promotes
791 regeneration of airway ciliated cells from basal stem cells. Proc Natl Acad Sci U S A *111*, E3641-3649.
792 10.1073/pnas.1409781111.
793 Tsarouhas, V., Senti, K.A., Jayaram, S.A., Tiklova, K., Hemphala, J., Adler, J., and Samakovlis, C. (2007).
794 Sequential pulses of apical epithelial secretion and endocytosis drive airway maturation in Drosophila. Dev
795 Cell *13*, 214-225. 10.1016/j.devcel.2007.06.008.
796 Villarino, A.V., Kanno, Y., and O'Shea, J.J. (2017). Mechanisms and consequences of Jak-STAT signaling in
797 the immune system. Nat Immunol *18*, 374-384. 10.1038/ni.3691.
798 Wagner, C., Isermann, K., and Roeder, T. (2009). Infection induces a survival program and local remodeling
799 in the airway epithelium of the fly. FASEB J *23*, 2045-2054. 10.1096/fj.08-114223.
800 Wagner, C., Uliczka, K., Bossen, J., Niu, X., Fink, C., Thiedmann, M., Knop, M., Vock, C., Abdelsadik, A.,
801 Zissler, U.M., et al. (2021). Constitutive immune activity promotes JNK- and FoxO-dependent remodeling
802 of Drosophila airways. Cell Rep *35*, 108956. 10.1016/j.celrep.2021.108956.
803 Weaver, M., and Krasnow, M.A. (2008). Dual origin of tissue-specific progenitor cells in Drosophila tracheal
804 remodeling. Science *321*, 1496-1499. 10.1126/science.1158712.
805 Xiao, C., Puddicombe, S.M., Field, S., Haywood, J., Broughton-Head, V., Puxeddu, I., Haitchi, H.M., Vernon-
806 Wilson, E., Sammut, D., Bedke, N., et al. (2011). Defective epithelial barrier function in asthma. J Allergy
807 Clin Immunol *128*, 549-556 e541-512. 10.1016/j.jaci.2011.05.038.
808 Yew-Booth, L., Birrell, M.A., Lau, M.S., Baker, K., Jones, V., Kilty, I., and Belvisi, M.G. (2015). JAK-STAT
809 pathway activation in COPD. Eur Respir J *46*, 843-845. 10.1183/09031936.00228414.
810 Zeidler, M.P., and Bausek, N. (2013). The Drosophila JAK-STAT pathway. JAKSTAT *2*, e25353.
811 10.4161/jkst.25353.
812 Zhang, X., Yue, P., Page, B.D., Li, T., Zhao, W., Namanja, A.T., Paladino, D., Zhao, J., Chen, Y., Gunning, P.T.,
813 and Turkson, J. (2012). Orally bioavailable small-molecule inhibitor of transcription factor Stat3 regresses
814 human breast and lung cancer xenografts. Proc Natl Acad Sci U S A *109*, 9623-9628.
815 10.1073/pnas.1121606109.
816 Zheng, X.J., Yang, Z.X., Dong, Y.J., Zhang, G.Y., Sun, M.F., An, X.K., Pan, L.H., and Zhang, S.L. (2016).
817 Downregulation of leptin inhibits growth and induces apoptosis of lung cancer cells via the Notch and
818 JAK/STAT3 signaling pathways. Biol Open *5*, 794-800. 10.1242/bio.017798.

819

820

821 Table 1 Genes that were highly upregulated in response to *Hop.CA* overexpression.

Name	Maximum group mean	Fold change	FDR p-value
CG16772	11.85	135.44	0
hop	286.06	35.43	0
CG14570	42.21	35.37	0
CG14147	55.31	32.88	0
Hsp70Bb	161.51	29.99	0
Ubx	200.46	23.51	0
pre-mod(mdg4)-I	1.12	18.67	2.22648E-06
IM14	11.46	15.14	3.80132E-07
IM4	26.43	14.97	1.74645E-12
CG14569	1576.88	14.73	0
IM2	7.26	14.47	2.01792E-06
CG5791	1.79	13.80	2.90502E-05
CG9121	3.41	11.54	0
IM1	7.16	10.97	7.52122E-05
CG11413	35.70	10.64	3.44242E-07
CG16710	2.13	10.32	1.72352E-07
CG31960	267.26	10.05	0
CG16789	1.45	9.46	5.58576E-09
CG6034	6.92	8.47	4.7943E-11
Ace	2.06	8.19	0
CG13059	9.90	7.58	1.33893E-06
CG31809	8.64	7.39	0
CG7203	9.41	7.21	8.66989E-09
Vha14-2	2.51	7.05	2.31024E-07
wb	7.35	6.69	0
Drs	8166.47	6.64	0
CG5778	3.20	6.61	0.000294835
CG3457	2.69	6.34	2.38755E-06
Lcp65Ad	9.93	5.79	2.58249E-08
lectin-22C	29.06	5.67	6.88538E-06
fuss	3.97	5.67	0
CG43333	2.39	5.63	1.48392E-09
CG18336	2.96	5.49	5.52167E-05

CG32563	3.06	5.35	0.000696584
FASN2	1.65	5.34	2.95545E-10
Cyp4d21	45.70	5.31	0
Obp57d	1.80	5.28	0.000102926
CG17560	2.31	5.22	0.000766701
CG5888	68.16	5.20	0

822 $p < 1\times10^{-4}$, fold change > 5, maximum group mean > 1. The list is restricted to 39 genes.

823

824 Table 2 Transcription factor-binding site motifs enriched in 41 highly upregulated genes.

Matrix ID	Matrix name	P-value
MA0023.1	dl (var.2)	0.000443261
MA0022.1	dl	0.00407113
MA0532.1	STAT92E	0.00794732
MA0450.1	hkb	0.00811969
MA0197.2	nub	0.0154201
MA0242.1	Bgb::run	0.0371696
MA0204.1	Six4	0.0443521
MA0444.1	CG34031	0.0488169

825 A total of 133 transcription factor profiles were used.

826

827

828

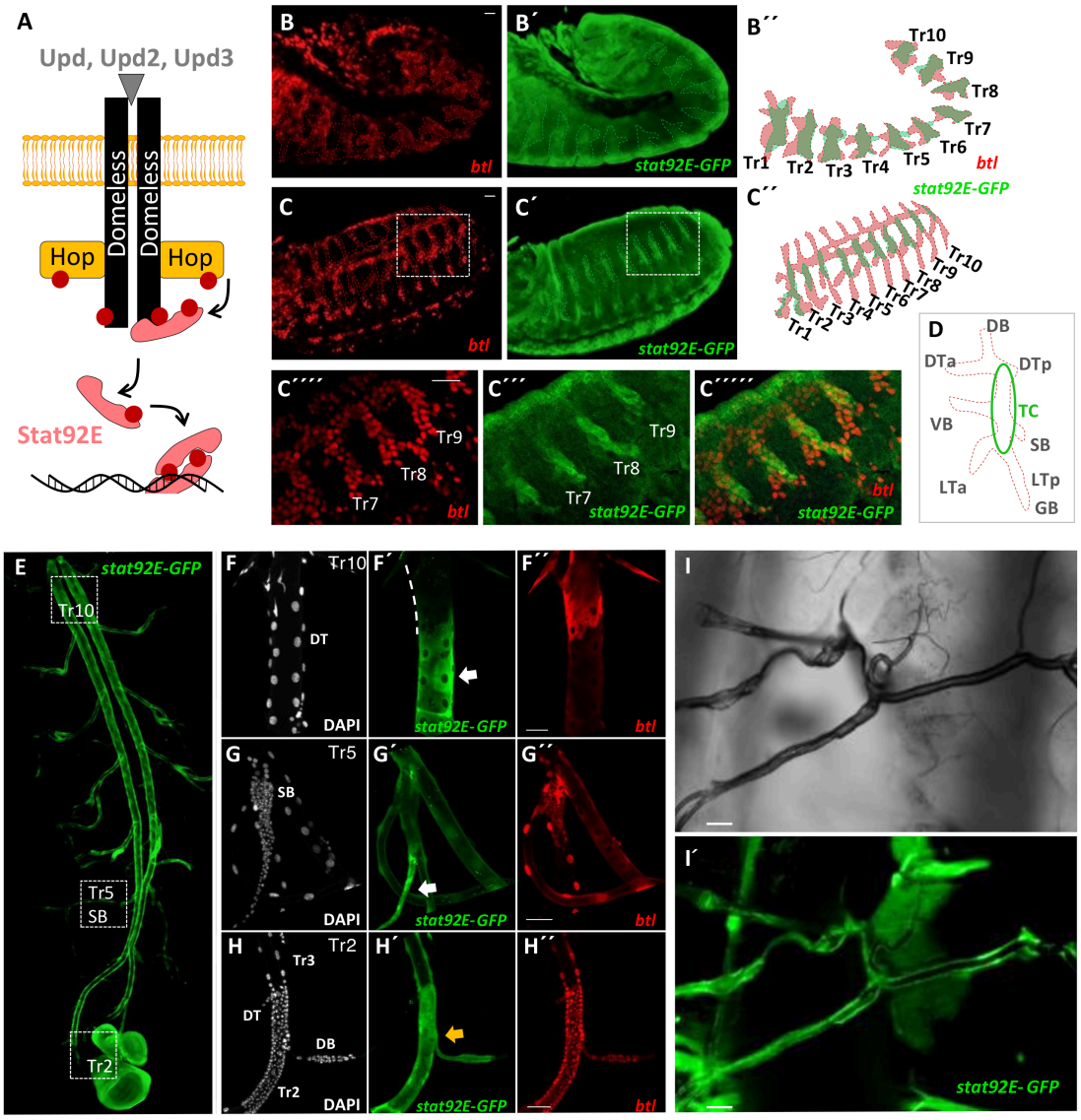

829

830 Figure 1: The activation of JAK/STAT signaling pathway in the respiratory system of *Drosophila*. (A)
831 shows a model of JAK/STAT signaling pathway in *Drosophila* comprising all major components. Three
832 ligands (Upd, Upd2 and Upd3) bind to a single receptor, Domeless (Dome), which transmits this
833 information via a single JAK (Hopscotch (Hop)) to a single STAT transcription factor (STAT92E). The
834 activation of JAK/STAT signaling through all developmental stages was detected by using a *STAT92E-*
835 *GFP* reporter (*btl-Gal4*, *STAT92E-GFP*; *UAS-LacZ.nls*). (B-D) Fluorescence micrographs of embryonic
836 trachea stained for GFP (green, JAK/STAT pathway activated zones), and beta-galactosidase (red,
837 tracheal metamere (Tr)), respectively. The activation of JAK/STAT pathway in the terminal regions is
838 weaker than that in the central regions before (B) and after the fuse of tracheal invaginations of all
839 segments (C). (D) shows the activation pattern of JAK/STAT signaling in the embryonic trachea
840 metamere. The stronger signal in the central region mainly belongs to TC (green circle). DB, dorsal

841 branch; DTa, dorsal trunk anterior; DTp, dorsal trunk posterior; VB, visceral branch; LTa, lateral trunk
842 anterior; LTp, lateral trunk posterior; and GB, ganglionic branch; SB, spiracular branch; transverse
843 connective, TC. The stronger signal in the central regions mainly belongs to TC. Scale bar: 20 μm. (E-H)
844 Fluorescence micrographs of larval trachea. JAK/STAT activity is present in most parts of the trachea
845 (E). The region in the posterior region of the trachea (dorsal trunk (DT) of Tr10, white dash line in F)
846 showed a decreased activity of JAK/STAT signaling compared to other tracheal epithelial cells. Scale
847 bar: 50 μm. Conversely, some regions like SB (G, marked by white arrow) and Tr2, DB (H, marked by
848 white arrow) showed an increased activity of JAK/STAT signaling compared to the tracheal epithelial
849 cells. Scale bar: 50 μm. (I) Fluorescence micrographs of adult trachea. JAK/STAT signaling was induced
850 in the trachea of the adult.

851

852

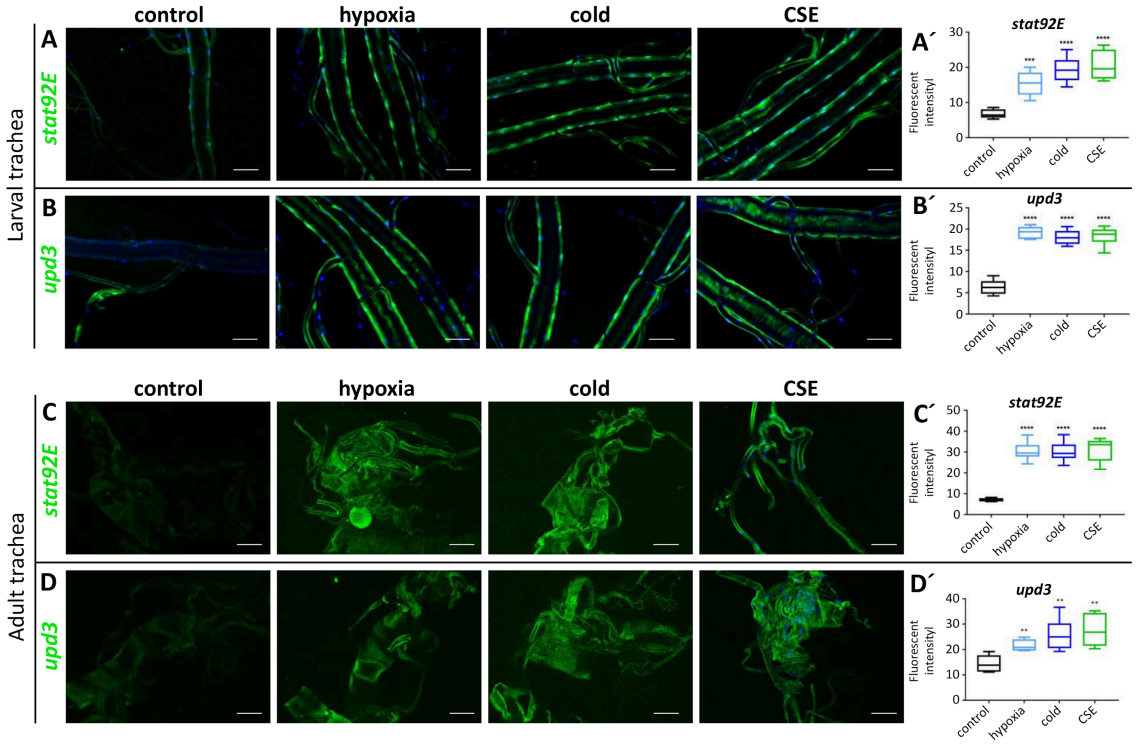

853

854 Figure 2: JAK/STAT signaling pathway in trachea was activated by external stimuli. (A and C)
855 Fluorescence micrographs of the trachea of *STAT92E-GFP* larvae (A) and adult (C) under normal
856 conditions and external stimuli, including hypoxia, cold air (cold), cigarette smoke exposure (CSE). The
857 external stimuli induced activity of STAT92E could be observed and was quantified through fluorescent
858 intensity (A' and C'). (B and D) Fluorescence micrographs of the trachea of *upd3-Gal4*; *UAS-GFP* larvae
859 (B) and adult (D) that were exposed to normal condition and external stimuli. The external stimuli
860 induced expression of *upd3* could be observed and was quantified through fluorescent intensity (B'
861 and D'). ** $p < 0.01$, *** $p < 0.001$, **** $p < 0.0001$ by Student's t-test. Scale bar: 100 µm.

862

863

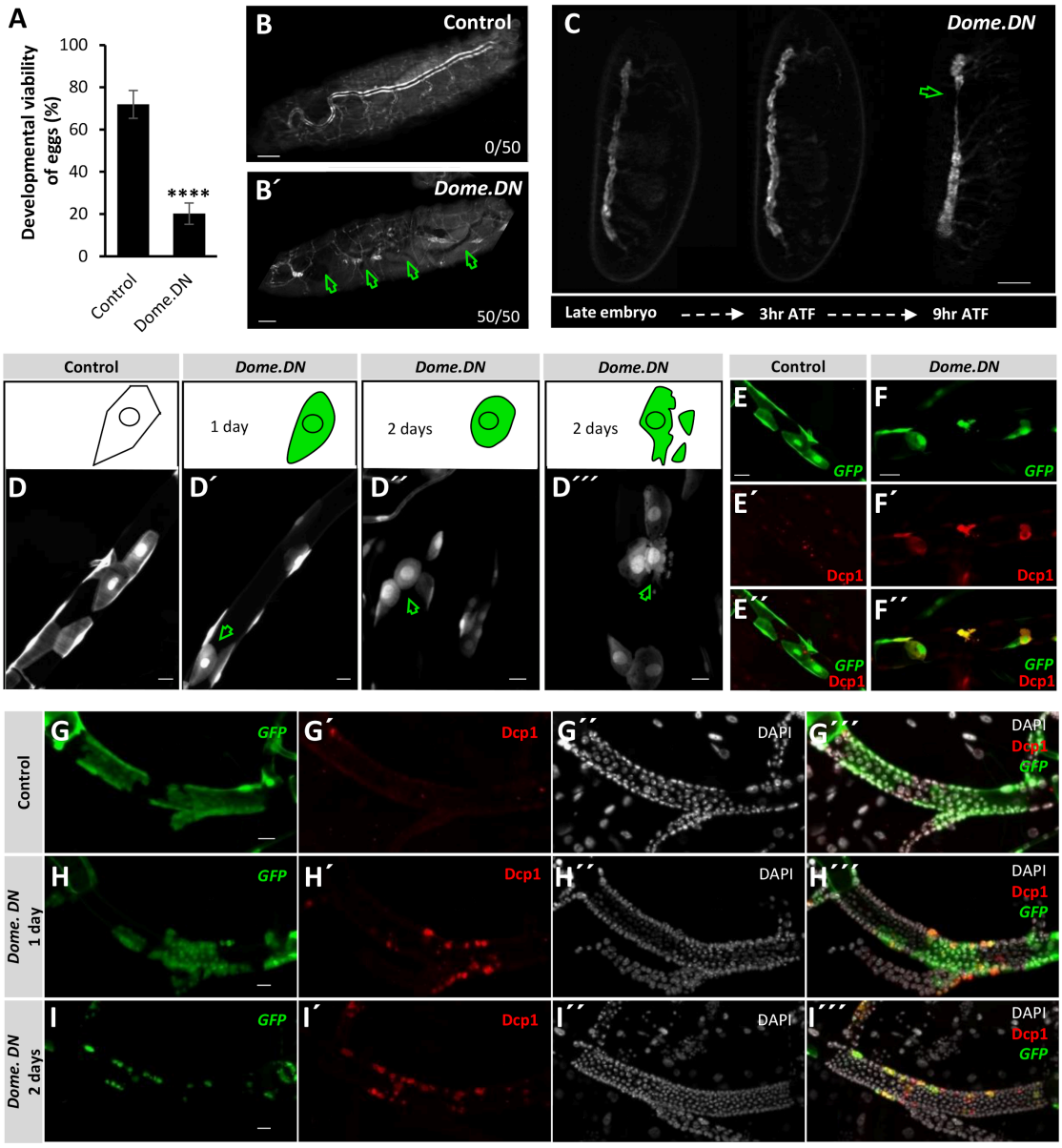

Figure 3: Inhibition of JAK/STAT signaling pathway induced epithelial cell apoptosis. (A) Ectopic blocking of JAK/STAT signaling in the trachea was done by expressing *Dome.DN* under the control of *btl-Gal4*. The developmental viability is shown by the percentage of embryos that hatched. (**** $p < 0.0001$ by Student's t-test). (B) Micrographs of surviving larvae. Scale bar: 50 µm. *Dome.DN* expression inhibited the formation of an intact tracheal tree. X/XX: emerged phenotype/total animals. (C) Time-lapse imaging of the trachea of *btl-Gal4>Dome.DN* embryos continuously for 9 hours after tracheal formation (9hr ATF). Scale bar: 50 µm. (D-I) Fluorescence micrographs of *Dome.DN* expressing mosaic mutant clones (GFP, green) in the larval trachea (*vvl-FLP, CoinFLP-Gal4, UAS-EGFP; tub-Gal80[ts]* (*vvl-coin.ts*)*>Dome.DN*). (D) Negative regulation of JAK/STAT pathway by expressing *Dome.DN* in the trachea led to changes in cell morphology (D' and D'') and disintegration afterwards (D''', green arrows, Scale

bar: 20 μm). (E-F) Fluorescence micrographs of the tracheal somatic cells of *vvl-coin.ts* larvae (E), and the tracheal somatic cells of *vvl-coin.ts>Dome.DN* larvae (F) stained for cleaved Dcp1 (red, on day 2 after induction). Scale bar: 50 μm. (G-I) The progenitor cells of Tr2 could be stained by cleaved Dcp1 earlier than the mutant somatic cells (red, on day 1 after induction). Scale bar: 50 μm. Nuclei are stained with DAPI.

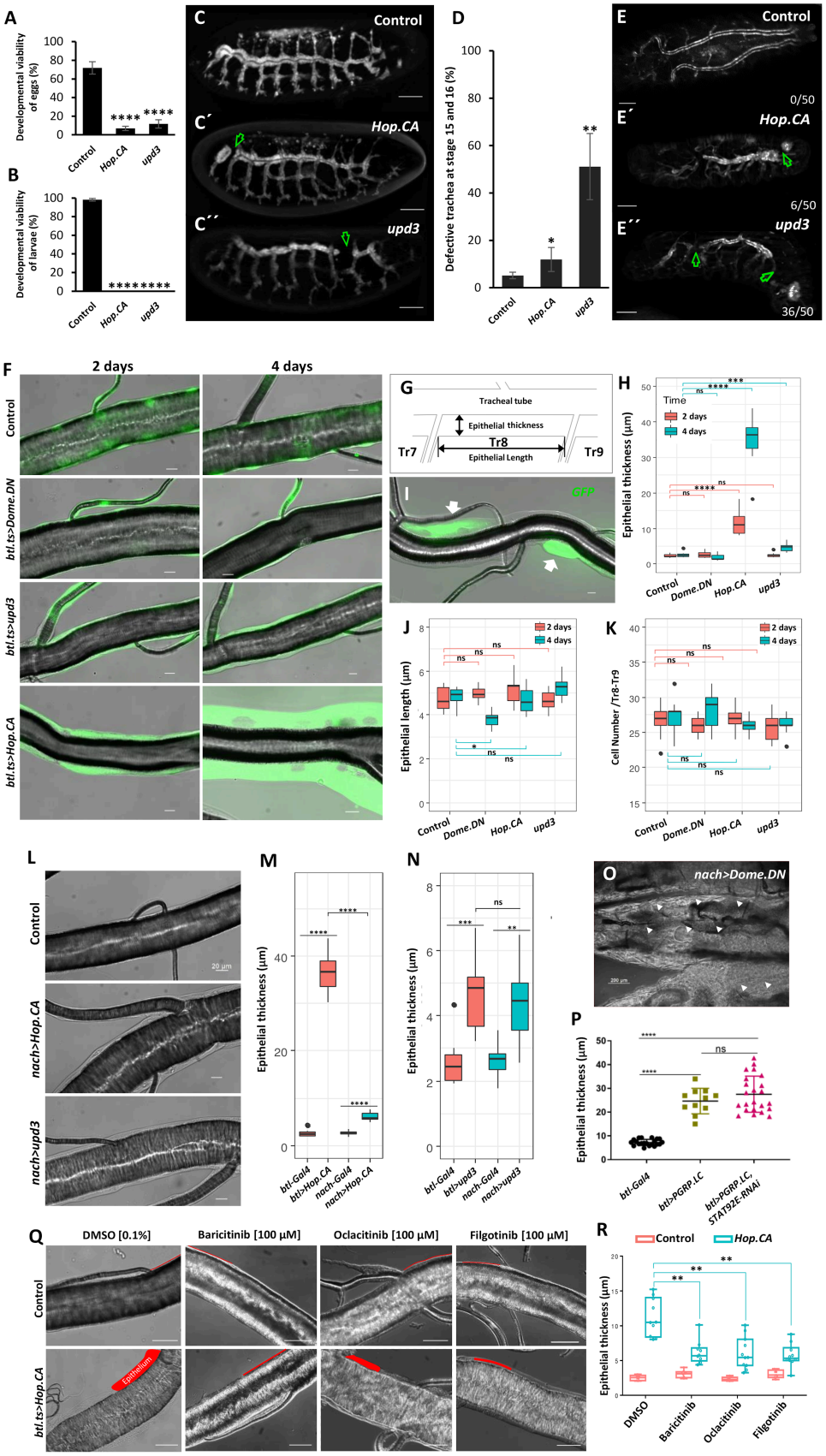

882

Figure 4: Ectopic activation of JAK/STAT signaling in the trachea induced cell thickening. Ectopic regulation of JAK/STAT signaling in the trachea was performed by expressing *Hop.CA* or *upd3* for activation and *Dome.DN* for inhibition of the pathway, under the control of *btl-Gal4*. The percentage of embryos that hatched (A) and the percentage of larvae that developed into pupa (B) are shown. (C) Fluorescence micrographs of *btl>Hop.CA* (or *btl>upd3*) embryos. Scale bar: 50 μm. (D-E) Activation of the JAK/STAT pathway in the trachea led to uncompleted tracheal development during tracheal morphogenesis. (D) Quantification of the numbers of defect trachea in *btl>Hop.CA* or *btl>upd3* embryos. (E) Micrographs of the trachea of the surviving larvae. Scale bar: 50 μm. (F) Ectopic activation of epithelial JAK/STAT signaling (*Hop.CA* or *upd3*) or inactivation (*Dome.DN*) under control of *btl.ts-Gal4* (dorsal trunk of Tr8 of L3 larvae). Larvae were raised at 29 ℃ for 2 or 4 days for induction, respectively. Scale bar: 20 μm. (G) Illustration of epithelial thickness, epithelial length. (H) Statistical analysis of the epithelial thicknesses in DT8 of the corresponding larvae. (I) Micrographs of DT8 of *vvl-FLP*, *CoinFLP-Gal4, UAS-EGFP* (*vvl-coin*)*>Hop.CA* larvae. Scale bar: 20 μm. The thickening of the tracheal epithelium is observed in those cells that express *Hop.CA* (arrows). (J-K) Quantification of epithelial length and the cell number of the DT8 region of larvae with different types of ectopic manipulation (including *Dome.DN*, *Hop.CA* and *upd3* expression in the trachea driven by *btl-Gal4, tubPGal80ts*) for 2 or 4 days, respectively. Mild activation of epithelial JAK/STAT signaling mitigated the thickening phenotype. (L) Micrographs of the DT8 regions of *nach-Gal4* larvae, *nach>Hop.CA* larvae and *nach>upd3* larvae. Scale bar: 20 μm. (M-N) Quantification of the epithelial thickness of the DT8 region of those larvae whose JAK/STAT signaling were activated by expressing *Hop.CA* or *upd3* under the control of *nach-Gal4* and *btl-Gal4*. (O) Micrographs of *nach>Dome.DN* larvae experiencing suppression of the JAK/STAT pathway make trachea translucent and filled with fluids. Triangle indicates the tracheal position. Scale bar: 200 μm. (P) Quantification of the epithelial thickness of the DT8 region of *btl-Gal4* larvae, *btl>PGRP.LC* larvae and *btl>PGRP.LC, STAT92E-RNAi* larvae. *TubPGal80ts* was used to inhibit the expression of *UAS-PGRP.LC* and *UAS-STAT92E*^{RNAi} before animal become L3 larvae and activated *UAS-* genes expression for one day. Changes in epithelial thickness could be rescued by application of specific JAK inhibitors (Q and R). (Q) Microscopy of the tracheal epithelium (L3 larvae). Control crossings *btl-Gal4, tubPGal80ts>w*^{1118} compared to JAK/STAT activated crossings *btl-Gal4, tubPGal80ts>Hop.CA*. Scale bar: 50 μm. (R) Quantification of epithelial thickness (highlighted in red) of the JAK inhibitors (Baricitinib, Oclacitinib, Filgotinib) compared to DMSO control. Green arrow: the defective region, ns means no significant, * $p < 0.05$, ** $p < 0.01$, *** $p < 0.001$, **** $p < 0.0001$ by Student's t-test.

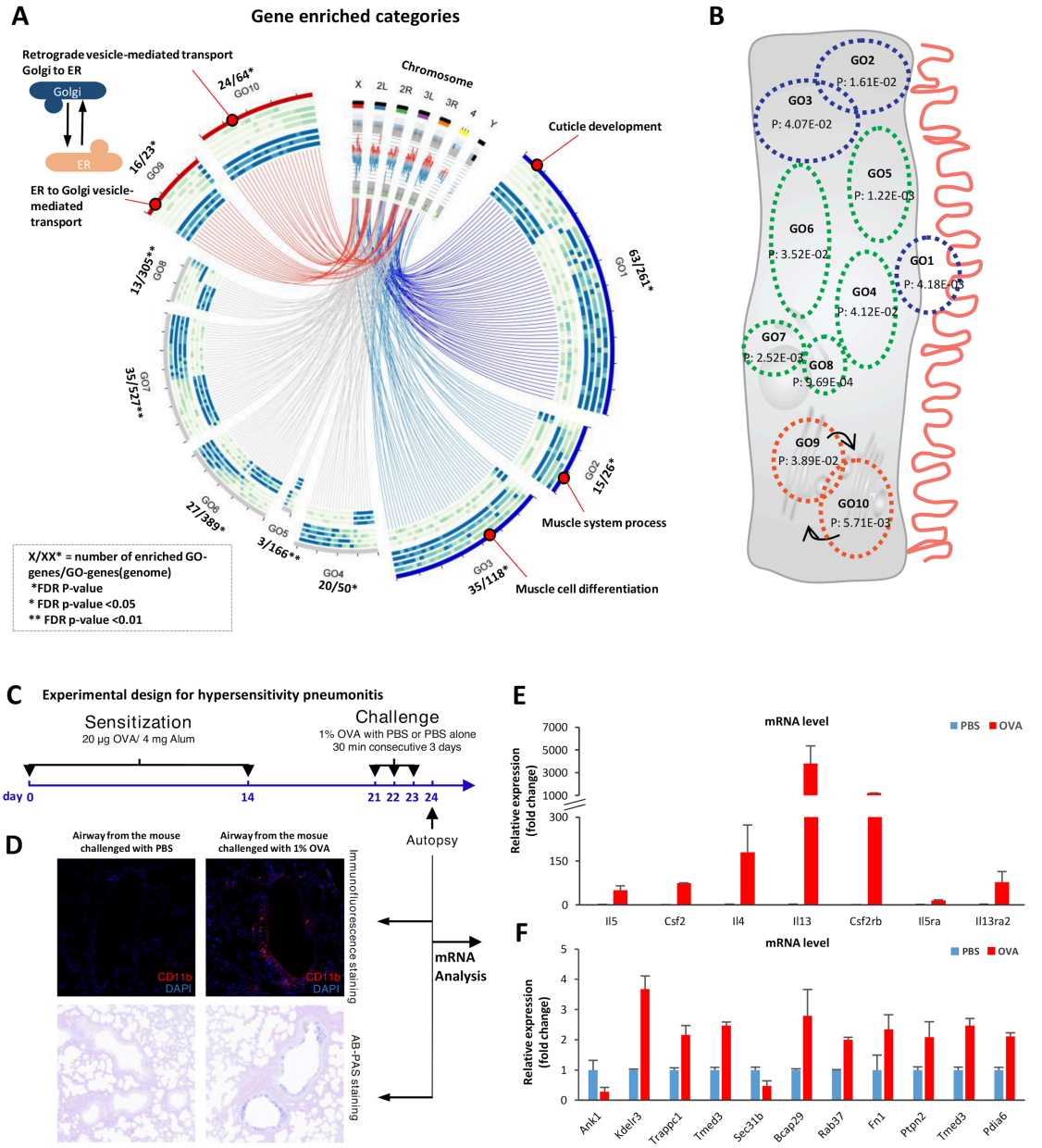

Figure 5: Gene Ontology (GO) enrichment analysis of the 2004 annotated differentially expressed genes in *Hop.CA* overexpressing airways *vs*. controls. (A) Gene ontology analysis showed 10 biological processes that were enriched in *Hop.CA* overexpressing airways compared with matching controls. Most regulated genes in the GO1, GO2, and GO3 were downregulated. Most regulated genes that involved in the COPI-and COPII-mediated vesicular transport between endoplasmic reticulum and Golgi (GO9 and GO10) were up-regulated. GO1, cuticle development; GO2, muscle system process; GO3, muscle cell differentiation; GO4, glutathione metabolic process; GO5, detection of chemical stimulus; GO6, cellular protein-containing complex assembly; GO7, RNA processing; GO8, translation; GO9, endoplasmic reticulum to Golgi vesicle-mediated transport; GO10, retrograde vesicle-mediated

transport Golgi to the endoplasmic reticulum. (B) Enriched biological processes were superimposed on a sketch depicting a tracheal epithelial cell, with the corresponding *p*-value added. Blue indicates processes where genes were mainly down-regulated; red indicates processes where genes were mainly up-regulated; green indicates processes where genes were both down-regulated and up-regulated to similar extents. (C) Experimental design for the OVA induced asthma model. Mice were sensitized with intraperitoneal injections of 20 μg of OVA emulsified in aluminum hydroxide in a total volume of 1 ml on days 7 and 14, followed by 3 consecutive challenges each day by exposure to OVA or PBS aerosol for 30 min. Mice were sacrificed 24 h following the final challenge. The left lungs were collected for histological analysis and the superior lobes were dissected for RNA analysis. (D) The lungs were stained with CD11b antibody and with the standard Alcian blue (AB) method followed by the Periodic acid–Schiff (PAS) technique. (E) Important chemokines and chemokine receptors induced by OVA aerosol are involved in JAK/STAT signaling pathway. (F) The genes that function in the process of ER to Golgi vesicle-mediated transport are mostly upregulated when the mice were exposed to OVA aerosol.

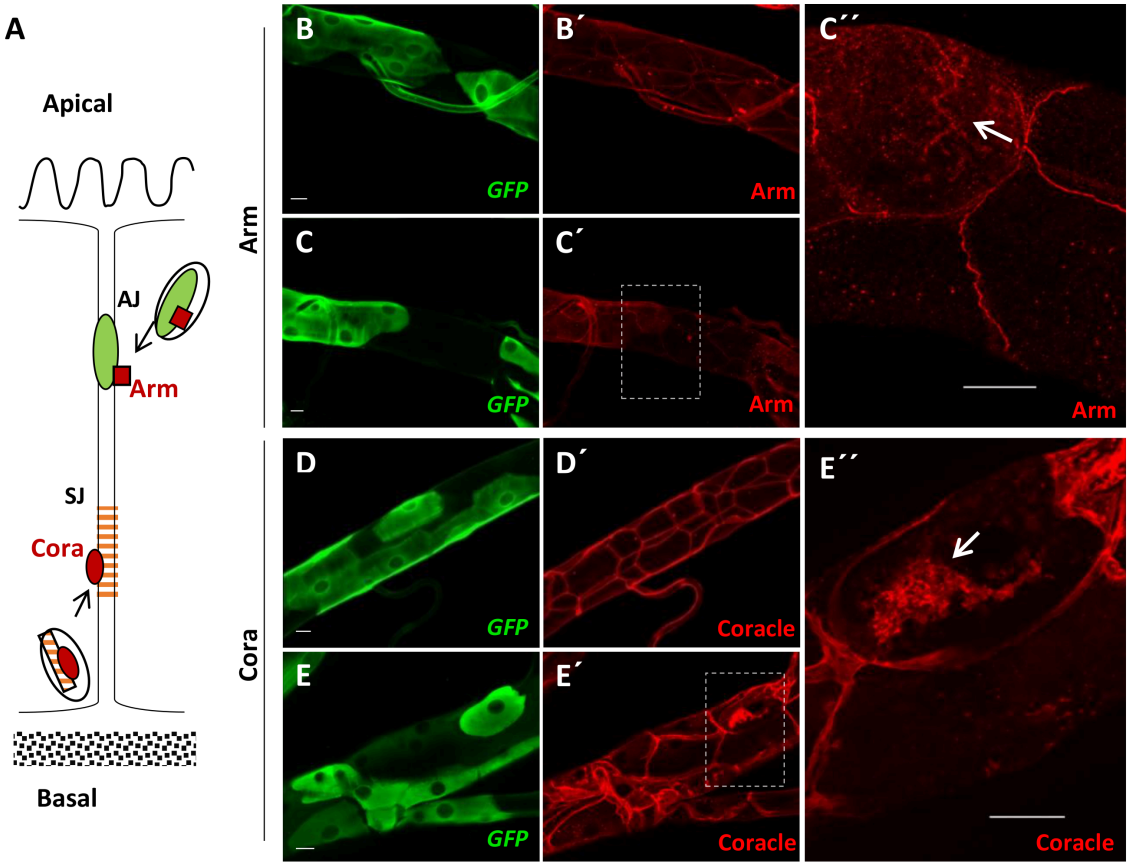

Figure 6: Activation of airway epithelial JAK/STAT signaling affects vesicle-mediated transport of proteins. (A) Schematic orientation of Arm and Cora at the contact zone between two airway epithelial cells. Adherens junction (AJ), septate junction (SJ). Trachea of *vvl-coin* larvae (control; B and D) and *vvl-coin>Hop.CA* larvae (treatment; C and E) stained for GFP (green, Gal4 positive cells), Arm or Cora (red), respectively. 30 specimens were investigated in each group. Scale bar: 20 µm.

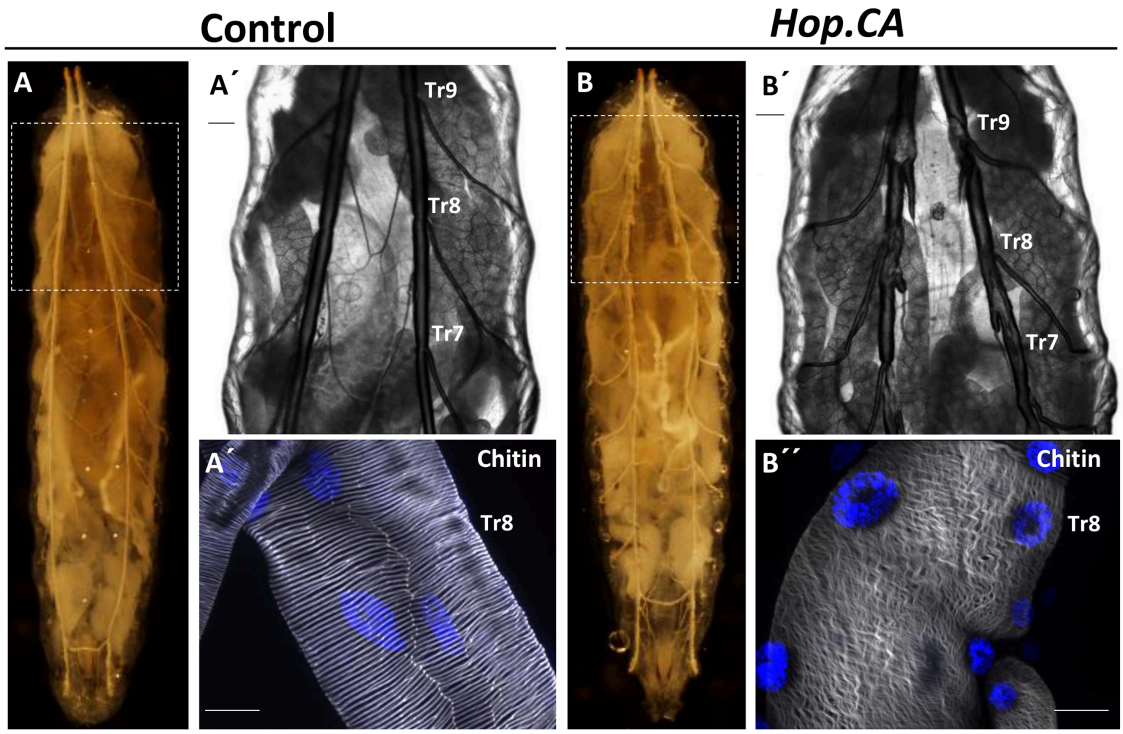

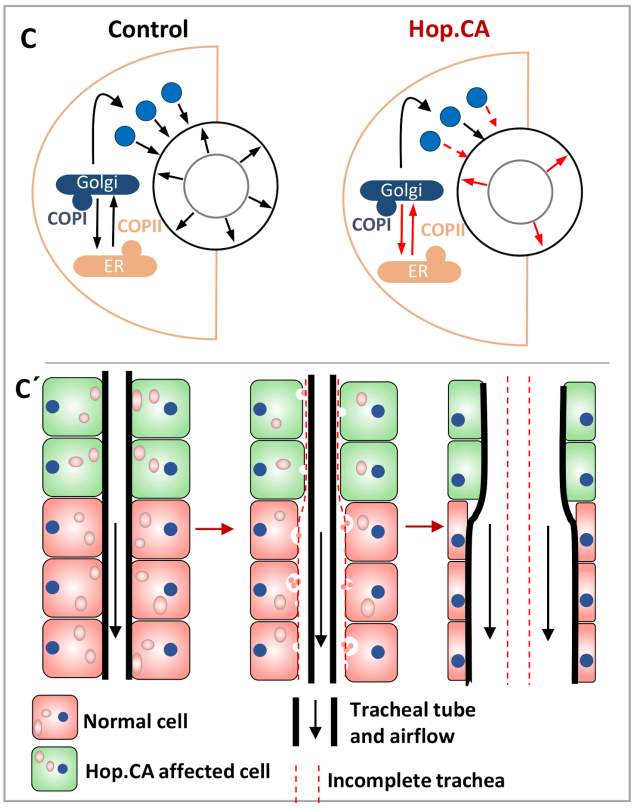

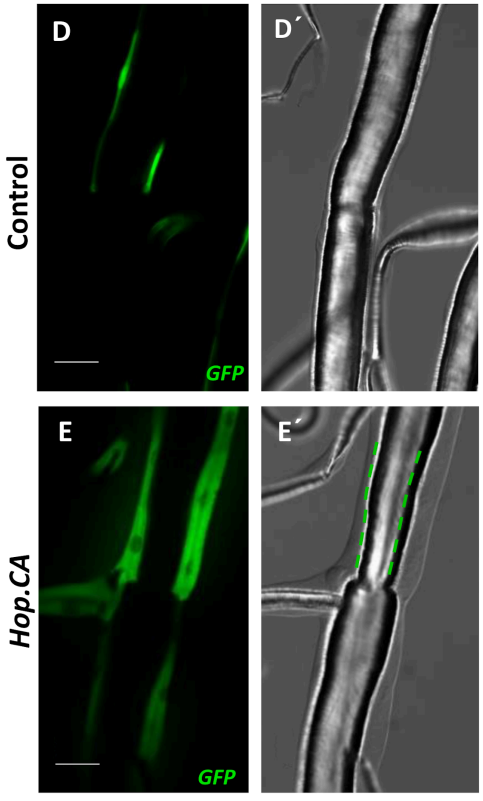

950

Figure 7: Activation of JAK/STAT signaling in airway epithelial cells affects the development of the epicuticle. (A-B) Activation of JAK/STAT signaling in airway epithelia observed in whole larvae by expressing *UAS-Hop.CA* under the control of the *btl.ts* (B-B'') compared to the control (A-A''). In (A' and B') the region containing Tr7-Tr9 is shown. (A'' and B'') Chitin staining of isolated airways (at the Tr8 region). Scale bar: 50 µm. (C) Schematic illustration of a potential explanation for the thickening of the epithelium and narrowing of the tube. In the control epithelium, a secretory burst of luminal proteins drives the diametric expansion of the tubes, and this process depends on vesicle-mediated transport. COPI-and COPII-mediated vesicular transport plays a central role in this process, mutation members in the process underly the tube size defect in previous reports (Jayaram et al., 2008; Tsarouhas et al., 2007). Although active JAK induced the expression of the genes involved in the vesicle-mediated transport, long-term activation eventually impedes the transport of vesicles out of the cell (C). This dysfunction of transport could lead to the appearance of tube size defects such as the increase in the cell volume and narrowing of the tube size (C') (Jayaram et al., 2008; Tsarouhas et al., 2007). (D-E) Micrographs of the trachea of *vvl-coin* larvae (control; D) and *vvl-coin>Hop.CA* larvae (treatment; E). Cells with *vvl-Gal* expression are stained with GFP (D-E). The green dash line in the E' show stenosis in the regions with cells expressing *Hop.CA* to a high degree. Scale bar: 50 µm.